Johanna Johnson

Aspects of Flexographic Print Quality and Relationship to some Printing Parameters

Johanna Johnson

Aspects of Flexographic Print Quality and Relationship to some Printing Parameters

Johanna Johnson. *Aspects of Flexographic Print Quality and Relationship to some Printing Parameters*

DISSERTATION

Abstract

Flexographic printing is a common printing method in the packaging field. The printing method is characterized primarily by the flexible printing plate and the low viscosity inks which make it suitable for use on almost any substrate. The object of this study was to obtain further knowledge of some important mechanisms of flexographic printing and how they influence the print quality. The thesis deals with printing primarily on board and liner but also on newsprint with water-borne ink using a full-scale flexographic central impression (CI) printing press. Several printing trials have been performed with a focus on the chemical interaction between the ink and substrate and the physical contact between the ink-covered printing plate and the substrate.

Multicolour printing exposes the substrate to water from the water-containing ink. The emphasis was to investigate the relation between print quality and water-uptake of the paper surface with heat and water. Printing trials was carried out on substrates possessing a hydrophobic, and also a rather hydrophilic surface using a regular commercial water-borne ink. The favorable effect which water or surfactant solution had on the hydrophobic substrate with regard to print mottle could depend on its surface compressibility in combination with the hydrophobic nature of its surface that could affect the wetting properties.

Conventional printing involves physical contact between plate and ink and between ink and substrate. A method for measuring the dynamic nip pressure using thin load cells is presented. Print quality was influenced by the plate material. A correction procedure taking into account the size of the sensor was developed in order to estimate the maximum dynamic pressure in the printing nip. An attempt was made to identify essential mechanical and chemical parameters, and also geometrical properties of the plate that affected print quality. Laboratory printing trials were carried out and a multivariate analysis was applied for evaluation of print density data. The impact of the plate properties on print quality was evident. The essential properties of the plate that influence print quality were the small-scale roughness and long-scale roughness.

Papers included in the thesis

I   Johnson, J., Rättö, P., Järnström, L., Lestelius, M. and Järnström, L. (2005): Interaction Between Water And Paperboard And Liner In A Flexographic Printing Press, TAGA Journal, vol. 1, pp. 110-128.

II   Johnson, J., Lestelius, M., Blohm, E., Rättö, P. and Järnström, L. (2008): The Interaction between Water and Liner and Newsprint in Flexographic CI-Printing Press, Paper presented at TAGA 2008: 60th annual conference, San Francisco, CA, U.S.A, 16-19 Mar. 2008.

III   Johnson, J. Rättö, P., Lestelius, M. and Järnström, L. (2003): Dynamic Nip Pressure in a Flexographic CI-Printing Press, TAGA Proceedings 2003: 55th annual conference, Montreal, QC, Canada, 14-17 Apr. 2003, pp 357-374.

IV   Johnson, J., Rättö, P., Lestelius, M. and Blohm, E. (2004): Measuring the dynamic pressure in a flexographic central impression printing press, Nordic Pulp and Paper Research Journal, 19(1), pp. 84-88.

V   Johnson, J., Andersson, C., Lestelius, M., Järnström, L., Rättö, P. and Blohm, E. (2008): Degradation of Flexographic Printing Plates and Aspects of Print Quality, submitted to Nordic Pulp and Paper Research Journal

These papers are included as appendices. Brief summaries of the results in these papers are presented in chapter six. Introductions to printing, flexographic printing, ink transfer and print quality evaluations are given in sections one to five. This latter section also gives general descriptions of the various experimental techniques and methods used in the Papers. The reason for not ordering the papers strictly chronologically is that this arrangement better describes the successive gain in knowledge during the progression of the work.

Johanna Johnson's contribution to the papers

Johanna Johnson performed all the experimental work with the exception of the static and dynamic surface tension measurements of model fluids and ink in Paper I, the Hg-porosity measurements in Paper I and II, the ink amount analysis using Atomic Absorption Spectroscopy in Paper I and III, the platen press trials in Paper III, the mathematical correction procedure in Paper IV, the ESCA analysis in Paper V and the surface roughness estimation of plates in Paper V. Johanna Johnson is the main author of these five papers.

Related reports by the same author

Nordström, J.-E. P. and Johnson, J. (2002): CSWWO (Cold set waterless web offset) using standard TMP/DIP newsprint, Presented at the 11th International Printing and Graphics Arts Conference, 1-3 Oct., Bordeaux, France.

Johnson, J. and Järnström, L. (2003): Moisture and print determine the quality: flexographic printing, Nordisk Papper och Massa, no. 2, pp 46-48.

Andersson, C., Johnson, J. and Järnström, L. (2008): Degradation of flexographic printing plates studied by thermal and structural analysis methods, submitted to Journal of Applied Polymer Science.

Table of contents

1 Introduction

Conventional printing is a complex process involving a periodic motion of two cylinders in close contact with each other and an ink acting as an interfacial material between the image carrier and the substrate. At the moment when the ink is transferred to the substrate, three components interact: the image carrier, the ink and the substrate. The performance of the image carrier is to a large content influenced by its chemical, mechanical and physical properties. The solidification of the ink on the substrate is highly dependent on the ink-paper interaction. The conditions in the printing process, such as printing speed and the force employed, also affect the ink transfer and the final print quality, as they affect the contact area and contact time. The printing press must be rapid and be stable to be cost-effective but it should also produce a satisfying print quality; overall it is the final appearance and functionality of the printed product that makes the printing process profitable.

Flexographic printing is distinguished from other print methods in the variety of substrates that can be printed on and it is therefore a central process in packaging printing, although gravure and offset are also used. Typical products printed by the flexographic printing process include paper, film and foil, multi-wall bags, corrugated and pre-printed linerboard, labels and wrappers, folding cartons, liquid board and cans.

1.1   Objectives

The overall objective of the work described in this thesis has been to learn more about the physical, mechanical and chemical processes that govern print quality in the flexographic printing process. Another important purpose of this study has been to investigate how different technical parameters in the printing process affect the final print quality.

The thesis includes five papers. Papers I and II are dedicated to study the effect of water-uptake of substrates, simulating the water in water-borne ink, including print mottle on solid tones, since full-tone areas are an

essential ingredient of overall print quality and printers claim that variations in reflectance in solid tones are one problem hindering a satisfying print result. Printing trials were carried out in a full-scale central impression flexographic printing press on uncoated substrates having different absorptivity properties. Results from Paper I concluded a reduction of print mottle on a hydrophobic substrate possessing fast water-uptake behaviour. Therefore, in Paper II, uncoated papers having a substantial water-uptake capacity were picked for the same investigation. The results from Papers II showed that there was no apparent influence on print mottle. The favourable effect of water pre-treatment seen on hydrophobic paper surfaces upon print mottle in Paper I could depend on the substrates surface compressibility together with its hydrophobic nature, which in turn may affect the wetting properties in a subsequent printing unit.

In Paper III, the dynamic nip pressure in the press was measured by means of thin load sensors and the consequences for print quality of using a soft or a hard plate were studied at different printing speeds and line loads. Even if the main deformation occurred in the sleeve the printing plate affected print quality as the soft plate transferred more ink to the substrate on a solid tone. This was explained by a better complying behaviour of the soft plate compared to the hard plate on the rough uncoated board. This investigation was extended in Paper IV considering the diameter of the pressure sensor compared to the nip length, and the maximum dynamic pressure was estimated, assuming that the pressure profile followed a cosine curve according to raw data from the sensor. The results showed that the maximum contact pressure and the nip length were quite similar for the two printing plates used in these trials. This was quite natural since the sleeve was by far the most compliant material.

In Paper V, the properties of flexographic printing plates were changed in a systematic and controlled way. The plates were characterized and printed with coated board in a laboratory press. The effect of plate properties on the print density was evaluated with the help of multivariate analysis. It was concluded surface topography of the plate take part in the amount of ink transferred to the substrate.

1.2 Paper and Paperboard

Paper has a good strength-to-weight ratio and is easily printed on by all printing processes. Paper can in essence be described as a layered structure containing fibres that are more or less compressed. Paper and board are made in a paper machine; the most essential parts of which are shown in Figure 1. Paper holds about 1 million fibres per gram (Fellers and Norman 1998). Depending on the paper properties desired, different types of fibres are used. There are basically mechanical (SGW - Stone Groundwood, RMP - Refiner Mechanical Pulp and TMP – Thermo-Mechanical Pulp) and chemical pulps, but also intermediate grades such as chemical mechanical pulp (CTMP - Chemical Thermo-Mechanical Pulp and NSSC - Neutral Sulphite Semi-Chemical). The mechanical pulps, which give high opacity, are used mainly in for newsprint production, and chemical pulps, which give high strength, for kraftpaper. Chemical Thermo-Mechanical Pulp is used in the middle layer of board for high bulk properties giving high bending stiffness. In addition to the fibres, fillers such as kaolin clay, chalk or talc may be added, and chemicals are added to aid the runnability in the papermaking process (Heinemann 2006).
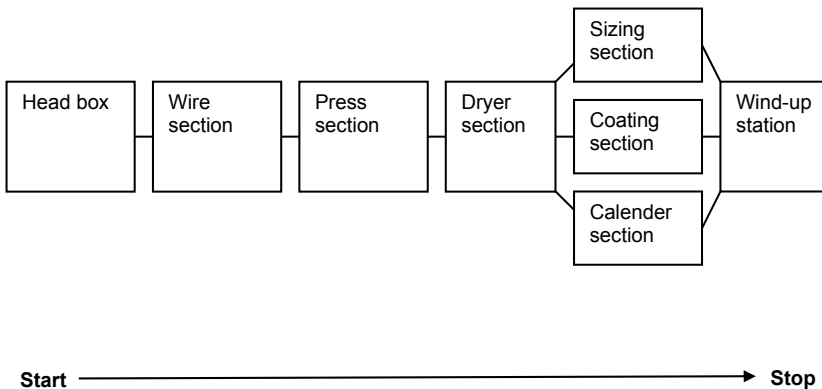
Figure 1. Basic stages of the paper-making process.

It is the paper surface that receives the ink. Therefore, the properties of the paper surface, its topography, compressibility, porosity and surface chemistry are of great importance (Fellers and Norman 1998). The

3

different stages in the paper-making process play important roles for achieving the desired surface topography of the paper and the fibers themselves exhibit irregularities on their surfaces. In the head box and during the formation on the wire section the fibers tend to aggregate and form flocs. Both the wire and the press-felt leave marks in the paper. In the dryer section, the paper web shrinks and this leads to waviness. The fibers, flocs, wire and felt marks and waviness are structural features of different length scales (Waterhouse 1995). Papers containing chemical pulp have a lower compressibility than papers made of mechanical pulp. Paper is both a fibre network and a network of pores. The absorption of water takes place by penetration into both pores and fibres. This is true for an unsized paper. In a sized paper the penetration of water takes place predominately in the fibres. Paper is usually coated and calendered to enhance its printing properties (Fellers and Norman 1998). Thick paper is called board. Most paper grades with a grammage less than 225 g/m^2 are defined as paper. Above 225 g/m^2, the paper is called board, but the designations overlaps (Tillmann 2006). Another definition is that paper exceeding a grammage of 170 g/m^2 is called board (Johansson et al. 1998). Depending on their use, paper and board may be grouped into four categories:

1. Graphic papers
2. Packaging papers and board grades
3. Hygienic papers
4. Specialty paper and board grades

Newsprint belongs to the graphic paper group. It consists primarily of a mixture of primary and secondary fibres (0-100 %). The primary fibres include SGW or TMP and a certain amount (< 10 %) of chemical pulp. The principal field of application is newspaper production. White top liner, liquid packaging board and test liner all belong to the family of packaging papers and board grades, where test liner is one of the bases for corrugated board and is produced in a variety of strengths, stiffnesses, wet strength and printability properties. Board grades are further divided into: cartonboard, container board and speciality board. Liquid packaging board belong to the cartonboard group and white top liner belongs to the container board group. Cartonboards are used mainly for consumer

product packaging such as food and milk and container boards (corrugated boxes) are used in many packaging applications from simple boxes for transportations and to multicolour printed displays for stores. Board grades have often a multilayer structure (Tillmann 2006).

1.3 Printing

Printing is a process for reproducing text and image on a suitable substrate with ink. The printing process can be either conventional or non-impact. Generally, the distinction between the technologies is that conventional printing uses a printing plate and non-impact does not use one. The most common non-impact technologies are electrophotography and ink jet (Kipphan 2001). Conventional printing is favoured for printing long runs. This saves costs because the price per product is less for a large quantity than it is for a short run. The machine used to transfer ink mechanically from a printing plate to a substrate is called a press. Gutenberg is reported to have invented the first conventional printing press during the 1450s. After that, numerous refinements have been made and different technologies have arisen. The different conventional printing technologies are divided into four main groups depending on the technique for ink transfer and image carrier, viz.: screen, lithography, gravure and letterpress printing (Kipphan 2001). Figure 2 provides a simplified view of the image carrier of the different printing methods. Letterpress printing (Figure 2d) is recognized by its raised hard printing elements. The high viscosity ink is transferred with a high contact pressure to the substrate.
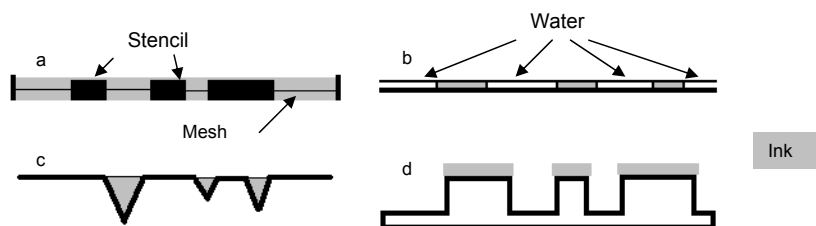

Figure 2. Image carriers and principles for different printing technologies, a) the print form for screen printing, b) the printing plate for lithographic printing, c) the printing cylinder for gravure printing and d) the printing plate for letterpress printing.

The focus in this thesis is flexographic printing, which evolved out of rotary letterpress printing, but instead of a hard printing plate a soft flexible printing plate is used. The viscosity of flexographic inks is lower than that of the inks used in letterpress printing. Another important difference is the contact pressure, which is less than in letterpress printing.

At first flexography was called aniline printing and the name persisted until 1951. Aniline printing, designed to run with a central impression cylinder and surrounding printing units, dates back from the 1890s. The name "aniline printing" originated from the aniline dyes used in the inks. The aniline dye was made of a coal tar derivative and was later banned from food packaging because of their toxicity (Herzau-Gerhardt 1999). The first patented aniline printing machine (1908) printed bags in-line with a bag-making machine (Cushdin 1999a). The ink-metering was achieved using two rolls, one for picking up the ink from the ink reservoir and another for doctoring the ink film and transferring it to a wooden or metal plate. The ink-metering system was coarse and difficult to control. In 1939, a mechanically engraved cylinder, the ink-metering roll or the so called anilox roll, was introduced to the aniline industry (Cushdin 1999a). This made ink-metering more accurate and the old rubber roll to rubber roll arrangement disappeared. The introduction of new substrates such as polyethylene (1940s) constrained the printing press manufacturers and ink suppliers to make more sophisticated web tension devices, drying systems and ink formulations. In the 1970s, the molded rubber plate was replaced by photopolymer printing plates. The introduction of photopolymerisation in the plate-making industry has led to a remarkable increase in print quality and has helped the growth of the flexographic printing industry (Kannurpatti and Taylor 2001). Today the flexographic process has become more computerised, not only computer control in the printing press such as impression setting, video inspection of the web, but the pre-press stage of the printing plate-making process is also controlled by computers (Cushdin 1999a).

1.4 The Flexographic Printing Process

The printing press configuration in flexography is dependent on the material to be printed. Available configurations are central impression cylinder system, in-line design and stack-type design. Central impression (CI) presses were originally developed for flexible packaging materials. In-line printing systems may comprise a separate unit for e.g. folding boxes. Stack-type presses are used only for simple printing jobs such as bags (Beier 2001). The central impression press see Figure 3, is the dominating design used today (Herzau-Gerhardt 1999).

Flexoprintingmachine SOLOFLEX®
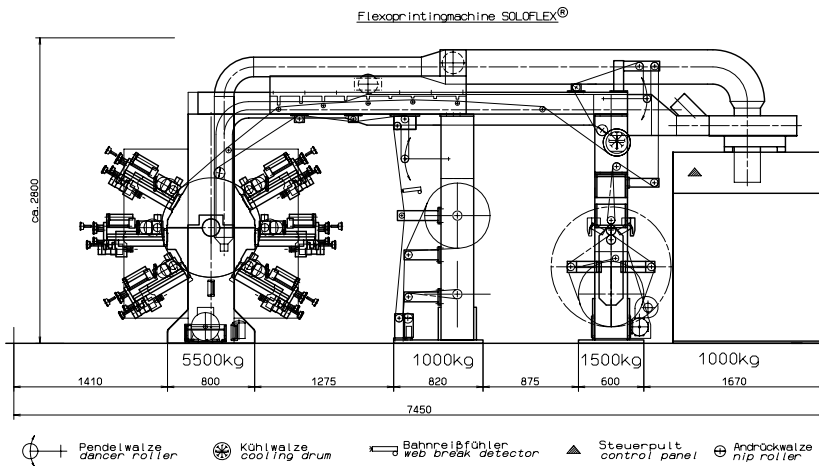
Figure 3. A central impression (CI) flexographic printing press (Soloflex8480, Windmöller & Hölscher, Germany). The unwind station is situated in the centre of the picture; on the left-hand side is the impression cylinder with surrounding printing units and on the right-hand side the rewind station. The paper web is led from the unwind position through the nips between impression cylinder and printing units and intermediate dryers. The paper then passes the main dryer before it is rewound. Source Windmöller & Hölscher manufacturer of printing presses.

1.5   CI-printing unit

Each printing unit in a central impression cylinder press consists of the central impression cylinder, an anilox roll and a printing plate cylinder (Figure 4). A CI press usually has six to eight units. Four units are dedicated to the CMYK process colours and the remaining are used for specific Pantone colours or lacquer. The ink metering system involves the anilox roll and an ink feeding arrangement. The ink feeding entity can be controlled by a chambered doctor blade system to which the ink is pumped from the ink tray.

1.5.1   The anilox roll

The primary role of the anilox roll is to transfer a finite amount of ink through small engraved cells via the printing plate to the substrate (Trungale 1997). The engraved cells have a shape of a truncated hexagonal cone with a specific volume (ml/m^2), and are distributed in a regular screen pattern over the anilox roll with defined numbers of lines/cm. An example is an anilox roll with 120 l/cm and a nominal ink capacity of 8 ml/m^2. The cell count/cm should be 4-5 times greater on the anilox roll than the cell count on the plate to print a dot of as small as 4 %. Generally the anilox has a core of steel, which can be plated with a thin layer of chrome or it can also be coated with ceramic.
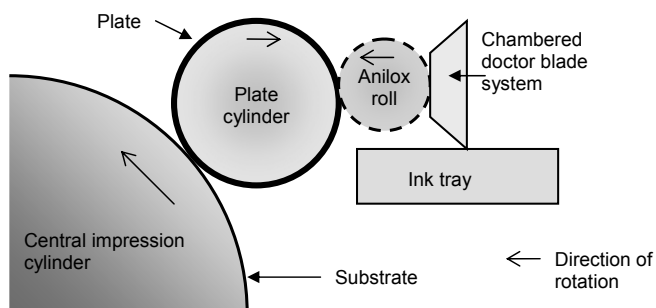
Figure 4. The major components in ink transfer using the flexographic central impression cylinder printing.

1.6   Inks

The flexographic technique can be used on a variety of substrates and the formulation of the inks depends on the process and printed matter. There are UV-curing and electron beam-curing inks, solvent-based and water-borne inks. The UV-curing ink needs UV-radiation to polymerise or dry it and electron beam curing is basically the same as UV-curing inks, however, they do not contain photoinitiators and need highly energized electrons to cure. In the simplest term, the solvent based and water-borne ink dry as the solvent evaporates or is absorbed in the substrate. As legislation demands a more environment-friendly ink, water-borne inks, which now contain only small amounts of volatile organic compounds (VOC), have become more frequently used for absorbent substrates (Sharpio and Sagraves 1997). The basic elements in flexographic inks are colorant, binder and solvent. Additives of various types are also used to impart printability and runnability on the press. Table 1 shows a typical formulation of a water-borne ink (Leach and Pierce 1999).

Table 1. Typical blue water-borne flexographic ink (Leach and Pierce 1999)

Component	[wt.-%]
50% Phthalocyanine Blue water paste (CI pigment Blue 15)	24.7
Acrylic emulsion	50.0
Water	20.0
Monoethylamine	2.0
Polyethylene wax compound	3.0
Organic defoamer	0.3

The colorant (50 % Phtalocyanine Blue water paste) is usually an organic pigment (CI pigment blue 15) and is dispersed in the binder. The binder (acrylic emulsion) keeps the pigment particles separated during the printing process and finally dries retaining the pigment on the printed matter. The solvent (water) dissolves the binder and keeps it stable through the whole process from manufacturer, storage and printing until the moment the ink dries on the paper surface (Liiri-Brodén et al. 1996). Polyethylene wax compound is added for rub resistance. Water-borne ink is prone to foaming problems therefore defoamers are put in (Leach and

Pierce 1999). Monoethylamine is used for making the insoluble caboxylated resins water-soluble at correct pH (Cushdin 1999b). Flexographic ink has a lower viscosity than the inks used in other letterpress methods. Most common procedure to measure and control the ink viscosity in flexo is with an efflux flow, for instance Ford, DIN or Zahn cup. The time it takes for a given volume ink to leave the flow cup in seconds is a measure of the ink viscosity. A normal reading of the ink viscosity could be 30 seconds using the Zahn cup No. 2.

1.7   Printing Plate

Three basic types of materials used in flexographic printing plate production are rubber plate formulations, liquid photopolymer media and solid-sheet photopolymers. Today the most commonly used plate material is the solid-sheet photopolymer material (Liu and Guthrie 2003) and this type of plate material has been used throughout this thesis. The print layout, half-tones and solid tones, is formed on the print plate. In multicolour printing there is one plate for each CMYK colour used. The half-tones in prints consist of tiny screen dots of each process colour that are intended to be small enough so that the human eye perceives a single colour. The solid-sheet plate has a design schematically illustrated together with the major components of the photo-sensitive layer in Figure 5.
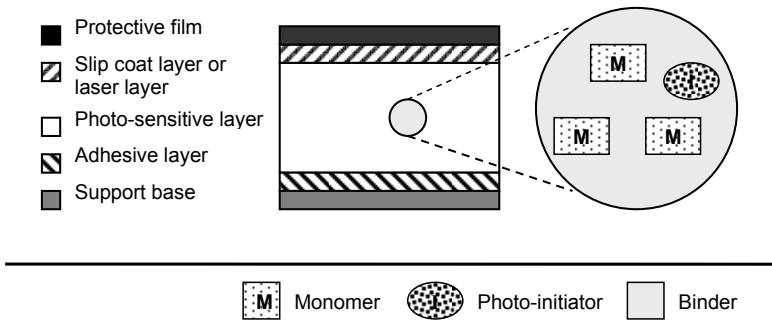
Figure 5. A general picture of photopolymer plate design and its major components in the photo-sensitive layer.

The plate build-up is characterised by multiple layers in a sandwich structure. Typically, there are five layers; protective film, slip coat layer, photo-sensitive layer, adhesive layer and support layer. Each layer has a special function and is custom-made to give the desired characteristics and contains different polymer materials. The protective film shields the plate from contamination and is removed prior to polymerisation. Underneath the protective film is the slip coat layer (for analogue exposure) or the laser layer (for digital imaging). Digital flexo do not require the use of a photographic negative film, since the photopolymer plate contains an integrated UV-opaque "mask" on its surface (Oum 2000). The mask is ablated on a computer-to-plate (CTP) thermal laser device, and the plate is subsequently polymerised with standard UV exposure lamps. The heart of the plate is the curable photo-sensitive layer, which creates the print layout when it is irradiated by UV-radiation with a specific wavelength. This layer also determines the thickness of the plate, which may vary from 0.127 to 6.35 mm (Liu and Guthrie 2003). An adhesive layer bonds the photo-sensitive layer with a support base for dimensional stability.

The major components in the photo-sensitive layer are the binder, monomer and photo-initiator. The binder also embeds the monomer and photoinitiator in the raw state and servers like a matrix. The binder is usually a solid thermoplastic elastomeric block copolymer which constitutes the backbone of the imaged plate. The liquid monomer is usually an ethylenic unsaturated acrylate compound and the liquid polymerisation initiator contains certain aromatic ketones (Liu and Guthrie 2003). Plate properties such as hardness can be controlled by the key ingredients and plasticisers. A common way to for a plate manufacturer to classify plates, apart from used the process used and the field of application is by hardness (°Shore A) and by thickness. The hardness (°Shore A) of the printing plates may be determined by a durometer. The hardness of the photopolymers may range from 34 to 85 °Shore A.

1.8   Pre-press process, plate-making, handling and storage

The photochemical pre-press process of flexographic photopolymer printing plates includes a number of stages when forming the print layout (Figure 6). These are: back exposure, main exposure, washing, drying and stabilization, post-exposure and light-finishing.
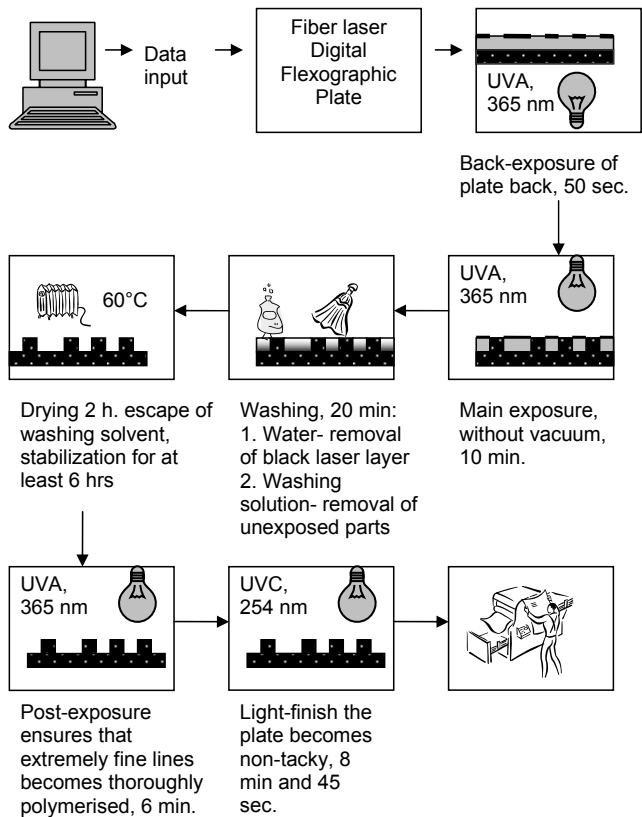
Figure 6. Example of the flexographic pre-press process for a "digital" printing plate (Paper V).

Consistency in plate-making has been pointed out by many to be the key point in establishing a proper printing plate for good print quality (Kenny 2004; Kannurpatti and Taylor 2001; Liu et al. 2002; Harri and Czichon 2006 and Galton 2003). Their handling, cleaning and storage are of great

importance to ensure and maintain good print quality. Storage and handling conditions have been investigated, and the positioning and exposure to light, electricity and temperature are factors that need to be controlled (Seckel 2003). In cleaning, solvent exposure is of great importance as it can produce effects like shrinkage, cracking and hardening (Stemper 1988 and Blair 2007).

1.8.1 Photopolymerisation process of the plate

The photopolymerisation of the plate starts with exposure to UV-A radiation of peak length 365 nm (Figure 7), which starts a radical chain reaction. **Initiation**: The light is absorbed by the photo-initiator (I) and the photo-initiator splits up to create radicals (R) (step 1a). The free radicals react with the monomer molecules, which in turn become reactive to other monomers (step 1b). **Propagation**: These reactive monomers react with other monomers and the polymer binder and form a crosslinked network (step 2). **Termination**: When two reactive molecules (monomers or radicals) react with each other, they form a deactive chain or section of the network (step 3). As long as the UV-radiation is switched on, and monomer is still left, the polymerisation continues and the propagation reaction dominates over the termination reaction (Kannurpatti and Taylor 2001).
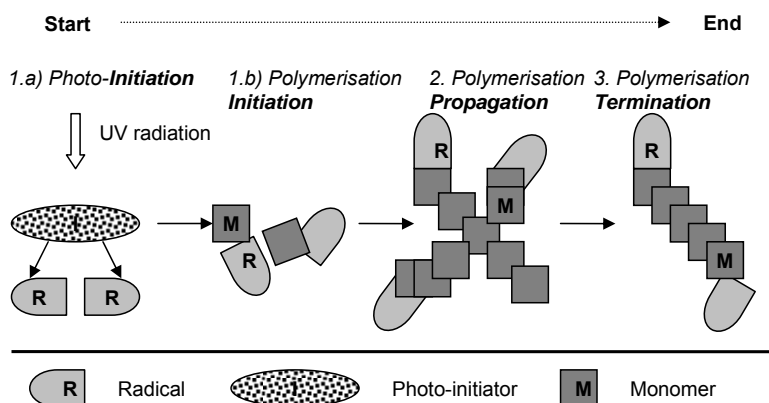
Figure 7. The photopolymerisation process.

2 Materials, characterizations and experimental techniques

2.1 Substrates

Two liquid packaging board grades A and B and one white top liner grade were chosen as substrates for the wetting and printing trials (Paper I). The liquid packaging board B was also used in Paper III. All substrates were uncoated. The liquid packaging boards consisted of five layers, two strong outer layers for strength and three middle layers that gave the board its thickness, bending stiffness and density. The print side was a blend of bleached short and long fibres, and the reverse side was unbleached long fibre, while the middle layers consisted of CTMP (Chemical Thermo-Mechanical Pulp), filler and reinforcement pulp. The white top liner had a similar build-up, but with only four layers. The substrates were all internally sized. The trials reported in Paper II were performed on standard newsprint (NP) and a white top test liner (TL). The NP was glazed on-line in the papermachine in a stack with three hard nips. The TL was produced from 100% post- industrial and post-consumer recycled fibres and was internally sized with starch. The top layer consisted of white post-consumer recycled fibres and 6% clay of the total weight. A clay-coated (double) board Performa Natura (StoraEnso, Imatra, Finland) with a grammage of 255 g/m^2 was used for the laboratory printing trials reported in Paper V. The base board consisted of a top layer of bleached sulphate pulp; a middle layer of bleached sulphate pulp and bleached CTMP (Chemical Thermo-Mechanical Pulp) and a back layer of bleached sulphate pulp. The substrate properties are summarized in Table 2.

Table 2. Properties of substrates.

Properties	Substrate					
	WTL	Performa Natura	A	B	NP	TL
Grammage, [g/m^2]	140	255	230	177	136	45
Surface roughness, [ml/min]	644	-	370	445	100	670
Thickness, [μm]	144	-	345	263	70	165
Surface Compressibility, [%]	14.7	-	17.0	13.8	2.5	4.2
Cobb$_{60}$, [g/m^2]	24	-	22	21	69	134
Surface Energy, [mJ/m^2]	47	-	44	40	43	49
Contact angle of water, [°]	102	-	117	117	62	47
Pore radius, [μm]	1.5	-	-	-	1.5	1.5
Porosity, [%]	34	-	-	-	-	-

2.2   Water-borne ink

A commercial water-borne cyan ink (Scanbrite, Sun Chemical, Stockholm) was used in the printing trials Papers, I-IV. The "viscosity" was determined with Zahn cup No. 2 according to ASTM D4212, and was kept constant at 30 (±0.1) seconds. The ink temperature was generally 22 (±1) °C. The dry solids content of the ink was 39 % and the density of the ink was 1079.5 kg/m^3. The ink contained 50-55 % water and had a Cu-content of 34 g/kg (dry ink).The newsprint in Paper II was printed with a water-borne cyan ink (Flexonews, Sun Chemical, United Kingdom) which had a surface tension of approximately 39 mN/m at 25°C, according to Wasilewski and Ernest (1986). The "viscosity" of the Flexonews ink was 20 seconds (Zahn cup No. 2). The cyan ink in Paper V was a water-borne ink (unicort process blue, Siegwerk Ink, Tampere, Finland). The "viscosity" was held constant at 23 sec using Zahn cup No.2. To maintain the ink viscosity constant in the different trials the ink was diluted with tap water, if necessary. The ink properties are displayed in Table 3.

Table 3. Ink properties of used inks in full-scale and laboratory printing trials

Properties	Ink		
	Scanbrite	Flexonews	Unicort process blue
Static surface tension, [mN/m]	32*	39**	-
Ink "viscosity", [sec.]***	30	20	23
Cu-content (dry ink), [g/kg]	34	-	-
Density, [kg/m^3]	1079	-	-
Dry solids content [%]	39	-	-

*Measurement performed at 23.9 °C
** at 25.0 °C according to Wasilewsky and Ernest (1986)
*** The time it takes for a given volume ink to leave the flow cup in seconds is a measure of the ink "viscosity".

2.3   Wetting agents

Tap water and three model fluids were used for humidification of the surface substrates during the printing trials in Paper I. Two of these three fluids were aqueous mixtures of water and surfactant and one was an aqueous mixture of surfactant, emulsified wax and alcohols. The surfactants employed were all non-ionic: Alkyl Poly Glycoside denoted APG (Estisurf GS40, Estichem A/S, Køge Denmark) with a short-chain alkyl group; an acetylene diol (Surfynol 402, Air Products Chemicals Europe, Utrecht, The Netherlands) here denoted AD and a surfactant solution/emulsion denoted SSE (Trapper Joe, Sun Chemical, Sweden) contained mainly acetylenic glycol but also other ingredients, such as emulsified wax and alcohols. The recommended dosage of SSE according to the supplier is 1 wt.-%. The surfactants and the SSE were mixed with water to suitable concentrations prior to the printing trials and the determination of surface tension. The following concentrations were chosen: APG 5 wt.-%; AD 0.1 wt.-% and SSE 0.5 wt.-%. In Paper I, the water-borne ink and model fluids were characterized with respect to their static surface tension according to the du Noüy method. A horizontal ring is pulled from the surface. The force F required pulling a ring with radius R from the surface may be related to the surface tension γ of the liquid by the equation:

$$F = 2(2\pi R)\gamma \qquad\qquad [1]$$

For a dynamic process like printing, the dynamic surface tension is more relevant (Bassemir and Krishnan, 1990). In Paper I, the dynamic surface tensions of the three model fluids were determined with the Maximum Bubble Pressure Tester (MPT2, Lauda, Germany). All model fluids possessed a rapid decrease in dynamic surface tension especially AD and SSE and reached their equilibrium value in less than 1 second. In Paper II, tap water and the acetylene diol (0.1 wt.-%), denoted Surfynol in the Paper, were used as wetting agents. In Table 4 the static surface tension (Du Noüy method) of the model fluids is displayed and the static surface tension for the ink is displayed in Table 3. The static surface tension of tap water was assumed to be 72.8 mN/m.

Table 4. Static surface tension at 20°C for model fluids and water used in the printing trials in Papers I and II.

Model Fluid	Static surface tension [mN/m]
Water	72.8*
APG (5 wt.-%)	35
AD (0.1wt.-%)	31
SSE (0.5 wt.-%)	29

*at 20 ºC according to van Oss (1994)

2.4   Ink and wetting agent delivery systems

The ink and wetting agents were transferred to the substrate using an ordinary ink transfer system; anilox roll, chambered doctor blade and printing plate. The model fluids in Papers I and II were applied to the paper web using a solid tone plate. To transfer different amounts to the paper, two anilox rolls were used. The model fluids and water were applied at two levels, "low" and "high". The "high" level was attained using an anilox roll with a 120 l/cm screen and cell depth of 20 μm and a nominal ink capacity of 8 ml/m^2. The "low" level was attained using an anilox roll with a 195 l/cm screen and a cell depth of 8 μm and a nominal ink capacity of 4 ml/m^2.

17

The ink was distributed using an anilox roll with 120 l/cm (cell volume 8 ml/m^2, cell depth 20 µm) for all substrates in Paper I and for TL in Paper II. An anilox roll with 250 l/cm (cell volume 6 ml/m^2, cell depth 15 µm) was used for NP in Paper II. In Paper V, an anilox roll with 180 l/cm and cell volume 6 ml/m^2 was for ink distribution in the laboratory printing trials. The anilox rolls used are described in Table 5.

Table 5. Anilox rolls used in the printing trials in Papers I-IV

Paper	Anilox rolls l/cm (ml/m^2, µm)		
	Ink	Model Fluid	
		low	high
I	120(8, 20)	195 (4, 8)	120 (8, 20)
II	120 (8, 20)	195 (4-4.5, 8)	120 (8, 20)
	250 (6, 15)		
III and IV	120 (8, 20)	-	-
V	180 (6, -)	-	-

2.5   Printing plate, tape and sleeve assembly

Two different printing plates, one "soft" and one "hard", were used in Papers I, III-IV. The printing plates had a similar build up with a light-sensitive photopolymer layer bonded to a polymer base. The "soft" printing plate was ACE (BASF, Germany) 1.14 mm with a hardness of 64° Shore A (according to DIN 53505). The "hard" printing plate was NOW (DuPont Cyrel, Germany) 1.14 mm with a hardness of 75° Shore A. The photopolymers were exposed to UV-radiation according to the straight light position (SLP) by Flexopartner AB (Sunne, Sweden). The layout consisted of full-tone areas and halftone areas of different tone values (30%, 50% and 70%) with a screen ruling of 28 l/cm. The soft printing plate was mounted on a soft coat sleeve (Polywest Kunststofftechnik, Germany) using a 0.1 mm (TESA, Germany), double-sided adhesive tape. The hard printing plate was mounted on a standard sleeve with a fairly soft plastic cell structure with a 0.5 mm cushion-foam tape (TESA, Germany). The printing plates were mounted with a microscopically controlled, one-piece plate mounter (DuPont Cyrel Microflex, Germany). Three Nyloflex printing plates (BASF, Germany) 1.14 mm, were used in Paper II. The plates had a hardness of 78 °Shore A. All the printing plates were mounted

on a soft coat sleeve (Polywest Kunststofftechnik, Germany). For two of the plates, a double-sided adhesive tape 0.2 mm (TESA, Germany) was used. These plates were used for ink transfer. The third plate was mounted with a similar tape but thinner, 0.1 mm, and was employed to transfer the model fluids. In Paper V, the printing plate was solid sheet digital Nyloflex® FAHD-II (Flint Group Printing Plates, Germany) with a thickness of 1.70 mm. This is a monolayer plate with a hardness of 69° Shore A. The plate, 1.70 mm thick, was mounted on a plate cushion 2.6 mm (Cycomp, DuPont, Germany), mounting foil Mylar film 0.35 mm (Cycomp, DuPont, Germany) and mounting tape 0.54 mm (Lohmann, Dalby, Sweden). Table 6 lists the properties of plates, tapes and sleeves used in the laboratory and full-scale printing trials.

Table 6. Properties of plates, tapes and sleeves used.

Paper	Plate	Thickness [mm]	Hardness [°Shore A]	Tape [mm]		Sleeve	
				adhesive	cushion	stand.	softcoat
I, III-IV	ACE	1.14	64	0.1	-	-	X
	NOW	1.14	75	-	0.5	X	-
II	Nylo.	1.14	78	0.1	-	-	X
		1.14	78	-	0.2	-	X
V	Nylo.	1.70	69	0.35	2.6+0.54	-	-

2.5.1 Changing the photopolymer plate properties

In Paper V, one set of printing plates was exposed to the normal pre-press process (Flexopartner, Sunne, Sweden) described in Figure 6, which contains main exposure (UVA 365 nm 10 min), post-treatment (UVA 365 nm 6 min) and light-finishing (UVC 254 nm 8 min 45 sec.) and was called normal exposure (denoted **norm. exp.**). Some plates were over-exposed with UVA or UVC in the normal pre-press process and denoted **2UVA**, **3UVC** and **4UVC**.

one time main exposure; 1×10 min UVA (**2UVA**)
two times light-finishing; 2×8 min 45 sec. UVC (**3UVC**)
three times light-finishing; 3×8 min 45 sec. UVC (**4UVC**)

19

Some printing plates were degraded using a QUV Accelerated Weathering Tester (Q-panel Lab Products, Bolton, UK) according to ASTM G 154 (cycle A) using direct radiation without window glass. The equipment is shown in Figure 22. One cycle subjected the plate for a total of 8 hrs UVA (340 nm) at 60°C and 4 hrs condensation at 50°C. The degradation was performed by (Polystatic AB, Ängelholm, Sweden).

Degraded in QUV:

1+1 hr with 4 hrs condensation at 50°C in between (**2h340**)
2+2 hrs with 4 hrs condensation at 50°C in between (**4h340**)
6+2 hrs with 4 hrs condensation at 50°C in between (**1cy340**)
6+8+2 hrs with 4 hrs condensation at 50°C in between (**2cy340**)

The treatments to which the degraded and over-exposed samples were subjected are shown in Table 7.

Table 7. Degradation and over-exposure processes for the printing plates in Paper V.

Prolonged exposure in the pre-press process		Radiation energy (MJ/m^2)					
		UV radiation	λ (nm)	Exposure time	UVA	UVC	Total
2×UVA	1×main exposure	UVA	365	10 min	1.87	0.49	2.36
3×UVC	2×light-finishing	UVC	254	2× 8 min 45 sec.	1.14	1.48	2.62
4×UVC	3×light-finishing	UVC	254	3×8 min 45 sec.	1.14	1.97	3.11
Exposure in the accelerated weather tester							
2h340	UVA exposure at 60°C	UVA	340	1+1 hr	2.86	0.49	5.08
4h340	UVA exposure at 60°C	UVA	340	2+2 hrs	4.59	0.49	8.54
1cy340	UVA exposure at 60°C	UVA	340	6+2 hrs	8.05	0.49	8.54
2cy340	UVA exposure at 60°C	UVA	340	6+8+2 hrs	14.96	0.49	15.45

2.6   Plate characterization

2.6.1 Topography

In Paper V, the roughness of the printing plate was evaluated with a MicroProf Chromatic Aberration Sensor (Fries Research & Technology, Bergisch Gladbach, Germany) with software Mark III. The arithmetic mean deviation of the surface area, sR_a, was used to describe the micro-roughness on the top of the dots and on the solid tone (Table 8). The R_a-values are calculated according to ISO 4287/1 and defined as:

$$R_a \approx \frac{1}{n}\sum_{i=1}^{n}|y_i| \qquad\qquad\qquad [2]$$

where y is the profile departure and n is the measured number of discrete profile deviations.

Table 8. SR$_a$-value for the normally exposed, over-exposed and degraded plates

Sample	Micro-roughness, sR_a, [µm]			
	20%	50%	70%	100%
Norm. exp.	0.044±0.004	0.050±0.003	0.051±0.003	0.039
2h340	0.049±0.006	0.045±0.004	0.053±0.003	0.024
4h340	0.055±0.006	0.065±0.002	0.075±0.004	0.065±0.015
1cy340	0.034±0.005	0.034±0.002	0.032±0.002	0.033±0.001
2cy340	0.023±0.002	0.036±0.003	0.028±0.001	0.019±0.002
2UVA	0.045±0.011	0.049±0.001	0.033±0.002	0.018
3UVC	0.055±0.005	0.059±0.003	0.056±0.003	0.028±0.001
4UVC	0.060±0.003	0.072±0.004	0.068±0.001	0.037±0.001

The sampling area varied with the dot diameter and the solid tone area was about 1×1 mm². The cut-off length was set to 10 µm and the noise filter to 2 µm. Micro-roughness was lowest for the most degraded samples (1cy340 and 2cy340) and highest for 4h340 and 4UVC. Other samples generally showed a micro-roughness similar to that of the normally exposed sample

Long-scale variations (no cut-off) were also measured using the roughness (R_a) along a line (Table 9), because a regular pattern (Figure 8) was

discovered, probably originating from the laser ablating device in the pre-press process (Figure 6, step 2). The line length varied and was about 0.30 mm for the solid tone and was shorter for the dots as the line length followed the dot diameter.

Table 9. R_a-value for the normally exposed, over-exposed and degraded plates.

Sample	Roughness, R_a, [µm]			
	20 %	50%	70%	100%
Norm. exp.	0.29±0.13	0.30±0.08	0.29±0.02	0.15±0.01
2h340	0.25±0.14	0.32±0.03	0.33±0.02	0.29±0.02
4h340	0.18±0.06	0.28±0.04	0.31±0.04	0.25±0.04
1cy340	0.22±0.06	0.35±0.07	0.27±0.03	0.16±0.01
2cy340	0.12±0.02	0.28±0.04	0.24±0.01	0.15±0.01
2UVA	0.16±0.04	0.18±0.03	0.15±0.05	0.12±0.02
3UVC	0.23±0.05	0.34±0.06	0.34±0.03	0.31±0.02
4UVC	0.25±0.08	0.35±0.00	0.35±0.02	0.29±0.02

The regular pattern had a peak-to-peak wavelength measuring approximately 95-100 µm (Figure 8). The waviness was also seen on the dot top area. Roughness, in terms of Ra-values, was lowest for 2UVA at all tone values. The other samples showed no increase or decrease in roughness valid for all the tone values relative to that of the normally exposed plate.
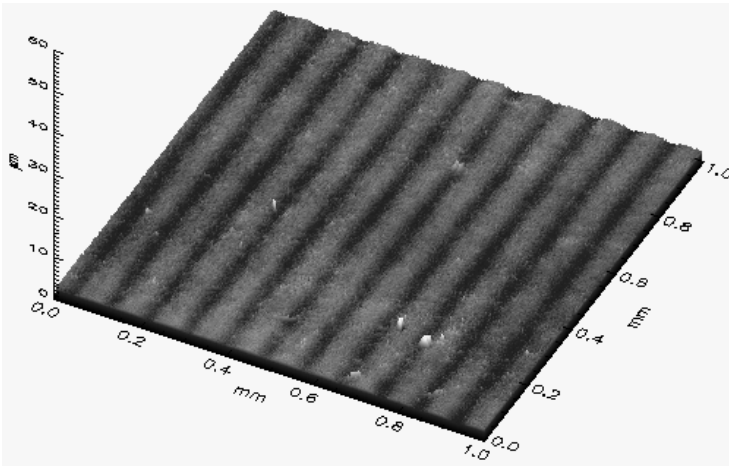

Figure 8. Regular stripes on a normally exposed plate originating from the fiber laser ablation step for digital plates (Paper V).

2.6.2 ESCA

In Paper V, the surface character of the printing plates was determined with ESCA (Electron Spectroscopy for Chemical Analysis) (Table 10-11). ESCA is a highly surface-sensitive and powerful tool for chemical surface analysis (Mark et al. 2005 and Etzler and Conners 1995). The ESCA method provides quantitative chemical information the chemical composition for the outermost 1-20 nm of a solid surface. When a material is exposed to a photon source, electrons contained in the material can be ejected if the energy of the incoming photon is greater than the binding energy holding the electrons within their orbital. Thus:

$$KE_e = 0.5mv^2 = h\nu - KE_B - W \qquad\qquad [3]$$

where KE_e is the kinetic energy of photoelectron, m is the mass of the electron, v the velocity of the electron, $h\nu$ the energy of incident photonbeam, KE_B the binding energy of the electron in its orbital, and W is the spectrometer work function (Istone 1995). ESCA provides quantitative data on both the elemental composition and the different chemical states of the element (different functional groups, chemical bonding, oxidation state, etc.). All elements e.g. (C, O, N, Si, Na and S) except hydrogen and helium were detected, and the surface chemical composition obtained is expressed in atom %. Prior to the analysis, the samples subjected to normal exposure and over-exposed were washed for 30 sec. under isopropyl alcohol, ethanol and water in that order. The degraded samples were washed during the UV-treatment in the QUV-chamber.

Table 10. Relative surface composition in atom %. Normally exposed was washed before the analysis. 4h340 and 2cy340 are washed during the treatment in the QUV-chamber.

Sample	Surface composition [atom%]					
	C	O	N	Si	Na	S
Norm. exp.	96.0±1.1	4.0±1.1	-	(<0.1)	-	-
4h340	96.2±6.0	3.8±4.9	-	-	-	-
2cy340	84.9±1.1	14.6±1.0	0.33±0.0	(<0.1)	-	-

-=signal at noise level (below about 0.1 atom%) and
( )=weak peak in detail spectra, signal close to noise level

Table 10 clearly shows that the surface of the degraded sample contained more oxygen than the sample before treatment in the QUV-chamber and also some nitrogen. High-resolution carbon spectra, with chemical shifts due to carbons in different functional groups with oxygen, are grouped into four types of carbon peaks in the table. The results in Table 11 show that both samples contained a high amount of unoxidised carbon (C1-carbon: C-C, C=C, C-H, C-Si functional groups). The 2cy340 sample contained high amounts of oxidised carbon in the outermost surface layer, with 17 % of the total carbon amount as C2-carbon, 4% as C3-carbon, and 2% as C4-carbon. The results indicate that sample 4h340 contained slightly more oxidised carbon than the normal exposed sample without QUV-treatment. The experimental scatter for the 4h340 sample was relatively high.

Table 11. Chemical shifts in high-resolution carbon spectra (with binding energy positions for each carbon peak, after adjusting C1-carbon to 285.0 eV as the reference value). The shifts were due to carbons in different functional groups with oxygen. Values were from curve fitting of different carbon peaks with the total amount of carbon=100%. Norm.exp. was washed before the analysis. 4h340 and 2cy340 were washed during the treatment in the QUV-chamber.

Sample	Share of chemical shifts for each carbon peak [atom%]			
	C1 285.0 [eV]	C2 286.5 [eV]	C3 287.8 [eV]	C4 289.1 [eV]
Norm. exp.	96.4±0.1	2.7±0.1	0.5±0.1	0.4±0.1
4h340	94.2±10.0	4.4±7.7	0.8±1.4	0.5±0.9
2cy340	77.2±1.2	17.4±0.5	3.6±0.4	1.8±0.3

Examples of functional groups:
C1: C-C, C=C, C-H, C-Si
C2: C-O, C-O-C
C3: O-C-O, C=O
C4: O-C=O

2.6.3 Surface energy of plate

The energy of a surface is most commonly quantified using a contact angle goniometer. To examine the surface energy of a material, drops of defined liquids (Table 12) are placed on the material surface and the contact angles of these liquids on the surface are determined.

Table 12. Examples of surface tension of liquids with defined Lifshitz-van der Waals (LW) interaction and polar interaction components (γ^+) and (γ^-) (van Oss 1994).

Liquids	Surface tension [mN/m]			
	γ	γ^{LW}	γ^+	γ^-
POLAR				
Water	72.8	21.8	25.5	25.5
Ethylene glycol	48.0	29	1.92	47
APOLAR				
Diiodomethane	50.8	50.8	0	0

The nature of a surface or the interfacial free energy for a solid/liquid system is often explained in terms of apolar Lifshitz-van der Waals and polar (Lewis acid-base) forces. As these components are additive, it is possible to state the surface free energy (van Oss 1994) as:

$$\gamma = \gamma^{LW} + \gamma^{AB} \qquad\qquad [4]$$

where LW refers to the Liftshitz-van der Waals interaction and AB to the Lewis acid-base interaction. The Lewis acid-base component can further be divided into

$$\gamma^{AB} = \gamma^+ + \gamma^- \qquad\qquad [5]$$

Figure 9 shows a droplet of a liquid on a plane surface. The contact angle (θ) is defined as the angle that is formed at the junction of solid-liquid interface (SL) and the liquid-vapour interface (LV). When the contact angle is >90° the surface is said to be hydrophobic.
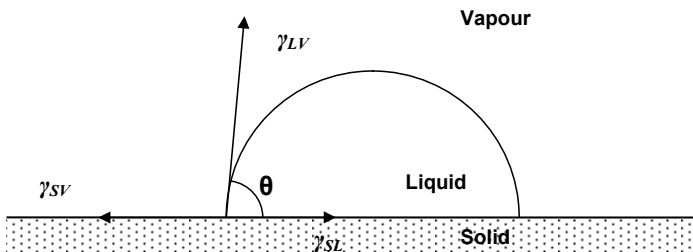

Figure 9. A schematic illustration of a water droplet on a flat solid surface

If the surface tension is considered to be a force along the perimeter of the drop, it is possible to write an equilibrium force balance of the drop:

$$\gamma_{LV}\cos\theta = \gamma_{SV} - \gamma_{SL} \qquad\qquad [6]$$

This is Young's equation which was qualitatively proposed by Thomas Young in 1805 (Hiemenz 1977). To calculate the solid surface energy (γ_S), the mathematical relationship from the Young–Dupré equation was used (van Oss 1994):

$$(1+\cos\theta)\gamma_L = 2\left(\sqrt{\gamma_S^{LW}\gamma_L^{LW}} + \sqrt{\gamma_S^+\gamma_L^-} + \sqrt{\gamma_S^-\gamma_L^+}\right) \qquad\qquad [7]$$

The surface energy of the plates in Paper V was determined by the acid-base method according to van Oss (1994) and shown in Table 13 using the FibroDAT instrument (Fibrosystem ab, Stockholm, Sweden), which enabled the contact angle to be measured as a function of time for a chosen substrate. Prior to the contact angle measurement, the normally exposed and over-exposed samples were washed for 30 sec. under isopropyl alcohol, ethanol and water in that order. The degraded samples were washed during the UV-treatment in the QUV-chamber. The lower surface energies of samples 2h340, 4h340 and 1cy340 in Table 13 were not expected, since the results from the ESCA analysis indicated a more oxidized surface the longer the exposure time in the accelerated weathering test. The surface energy was similar to that of the normally exposed sample before washing, indicating that all the surface contamination had not been removed by the accelerated weathering test, with the exception of the longest exposure time.

Table 13. Total surface energy (γ_{Tot}) of the printing plates and their apolar (γ^{LW}) and polar (γ^{AB}, γ^{+} and γ^{-}) components at a temperature of 22(±0.6) °C and a rel. humidity of 55(±1) %.

Sample	Surface Energy [mJ/m²]				
	γ_{Tot}	γ^{LW}	γ^{AB}	γ^{+}	γ^{-}
Norm. exp.	41.35	39.10	2.25	1.05	1.20
2h340	26.86	26.85	0.01	0.00	0.02
4h340	26.30	26.28	0.02	0.00	0.03
1cy340	25.24	25.13	0.11	0.05	0.06
2cy340	42.62	39.61	3.01	0.69	3.28
2UVA	40.47	39.10	1.37	0.47	1.00
3UVC	41.97	40.60	1.37	1.00	0.47
4UVC	41.09	40.60	0.48	0.11	0.54

2.6.4 Hardness of printing plate

The hardness, °Shore A, of the printing plates (Paper V) was measured by an analogue Durotech durometer MDS MD-1 (Ray-ran Test Equipment Ltd., Warwickshire, England, Great Britain) in accordance with ISO 7610. The hardness is shown in Table 14. The hardness increased with increasing UV-radiation.

Table 14. Hardness values of the printing plate samples

Sample	Hardness [°Shore A]
Norm. exp.	69.0±0.0
2UVA	71.8±0.3
3UVC	71.0±0.0
4UVC	71.2±0.3
2h340	74.7±0.6
4h340	74.3±0.3
1cy340	76.0±0.0
2cy340	77.7±0.6

2.6.5 Dot shoulder and dot area

Replicas, inverse 3-D-structures of the print layout (Figure 10), were prepared using two-component Silicon Rubber RepliSet-GF1 (Struers,

Ballerup, Denmark). The replicas were used to investigate the dot shoulder angle of the dot. The dot shoulder angle is here the angle between L1 and L2 in Figure 10.
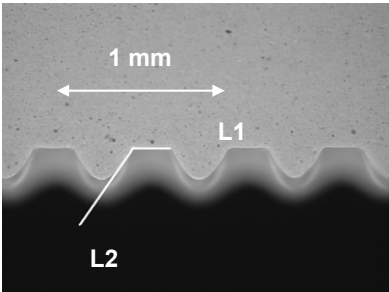

Figure 10. Replica of a printing plate showing the inverse cross section of a normally exposed plate with 20% tone value. The angle between L1 and L2 is the dot shoulder angle.

Pictures of the replicas were taken using a light microscope Axioplan2 (Zeiss, Stockholm, Sweden) picture capture with CCD-camera and software Optimate v.6.5 (Parameter, Stockholm, Sweden). The angle was measured using the software Image Pro Plus (Parameter, Stockholm, Sweden) Table 15.

Table 15. The dot shoulder angle for the normally exposed, degraded and over-exposed plates at different half-tones.

Sample	Dot Shoulder angle [°]		
	20%	50%	70%
Norm.exp.	121.5±2.5	130.2±2.5	134.9±3.4
2h340	123.0±2.7	127.9±1.8	132.1±2.5
4h340	123.9±1.4	127.2±1.3	132.7±2.3
1cy340	122.5±2.6	127.0±2.1	134.3±2.0
2cy340	121.4±2.2	130.6±2.4	133.2±2.0
2UVA	124.9±0.9	127.8±2.5	128.3±2.3
3UVC	121.8±2.3	127.1±2.0	132.1±2.8
4UVC	118.7±2.2	124.5±2.4	125.8±2.5

The light microscope, CCD-camera and the software Optimate v.6.5 was also used for taking pictures on dots on the printing plate. A magnification of 50 times was used for the most measurements; in certain cases, a

magnification of 100 times was used. Image Pro Plus was used to determine the dot area on the printing plate (Table 16). The red colour of the normally exposed printing plate changed to yellow when it was exposed to UV-radiation. This also occurs in the normal pre-press process, and is due to the decomposition of the azo dye (Neumann, 2008). The images were transformed to gray scale before a manual threshold of the gray level was set, since the individual printing plates differed in colour.

Table 16. Dot area for normally exposed, degraded and over-exposed printing plates at different tone values.

Sample	Dot area, [$10^{-3} \times mm^2$]		
	20%	50%	70%
Norm.exp.	13.0±0.2	36.2±0.4	53.3±0.5
2h340	12.8±0.2	35.5±0.4	53.4±0.5
4h340	12.2±0.3	34.9±0.5	52.8±0.7
1cy340	12.2±0.3	34.7±0.3	51.9±0.6
2cy340	12.1±0.2	34.1±0.3	52.6±0.6
2UVA	13.1±0.3	36.4±0.4	54.2±0.5
3UVC	13.2±0.2	35.9±0.5	53.7±0.4
4UVC	13.5±0.2	36.4±0.3	53.7±0.5

There was a tendency for the degradation to reduce the dot area of the printing plate regardless of tone value, and over-exposure tended to induce the dot area of the printing plate (Table 16).

2.6.6 Platen press trials

In Paper III, the platen press experiments were performed with equipment from MTS, Material Testing System, using two plates (65×65 mm²). Pressure was applied with a hydraulic cylinder. The "hard" and "soft" printing plates and the sleeve had approximate E-moduli of 280 MPa, 420 MPa and 10 MPa, respectively, at a frequency of 100 Hz, which corresponds to a pulse time of 0.01 sec. using a haversine pulse.

2.7 Paper characterisation and interaction with fluids

2.7.1 Roughness and compressibility of papers

The Parker Print-Surf (PPS) roughness tester (Lorentzen & Wettre, Stockholm, Sweden) was used to evaluate the roughness and compressibility of uncoated paper in Papers I-IV (SCAN-76:95). It is an air-leak roughness instrument in which an equation is applied to give the mean surface void in micrometers. The ratio of the PPS roughness values at 1 MPa and 2MPa clamping pressure was used as a measure of the surface compressibility and was calculated as

$$K = -\frac{dR}{dP} \tag{8}$$

where R is the roughness under applied pressure P (Bristow 1982).

2.7.2 Surface energy of papers

In Papers I and II the FibroDAT instrument (Fibrosystem AB, Stockholm, Sweden) was used to determine the surface energy of the substrates (Table 2). The determination was performed according to the acid-base method proposed by van Oss (1994) and discussed earlier in section surface energy of plates.

2.7.3 Pore size, porosity and absorption into pores

In Papers I and II, the dominant pore radius of a paper was estimated through mercury intrusion porosimetry (Dullien 1992). The measurements were performed with an AutoPore III instrument (Micromeritics, Norcross, GA, U.S.A.). In Paper I, the porosity, ε, of WTL was calculated as,

$$\varepsilon = \frac{V_{Void}}{V_{Total}} \tag{9}$$

where ε, is the porosity, V_{void} is the cumulate sample volume filled with Hg multiplied with the sample weight and V_{total} is the sample volume. In Paper I, the absorption of a liquid in a pore was described by the Poiseuille's and Lucas-Washburn equations. If an external pressure is taken into account, Poiseuille's equation may be utilized:

$$\frac{dh}{dt} = \frac{r^2 \Delta P}{8\eta h} \qquad [10]$$

where dh/dt is the rate of absorption, r the pore radius, ΔP the external pressure, η viscosity of the liquid and penetration length, h. The pressure in the printing nip can also contribute to increase the portion of ink that penetrates the porous substrate. The capillary absorption of a liquid in a pore was described by the Lucas-Washburn equation:

$$\frac{dh}{dt} = \frac{r\gamma_{LV} \cos\theta}{4\eta h} \qquad [11]$$

where dh/dt is the rate of absorption which depends on the contact angle θ between the liquid and the pore wall, the pore radius r, the surface tension of the liquid-vapor γ and the viscosity η. The pore size and porosity are displayed in Table2.

2.7.4 Fluid interaction with papers

The hydrophobic character of the papers (Papers I and II) was measured using the Cobb$_{60}$ method (SCAN-P12).The Cobb value is defined as the amount of water in g/m^2 that is absorbed over the test area under a pressure of a water pillar of 10 mm during a specified time (60 sec.). The Cobb-values of the substrates are shown in Table 2. In Papers I and II, the absorption of liquids under short contact times (0-2 sec.) was studied using the Bristow Absorption Tester (Bristow 1967; Lyne and Aspler 1982). The method is described in detail in Bristow (1967), but in brief it is a wheel with a circumference of one metre, which rotates at different speeds. A holder, which contains the liquid, is placed on the rotating wheel and the liquid (with addition of a dye) is spread through a gap onto the substrate

attached to the wheel. The length of the track left by the liquid is dependent on the substrate roughness and absorptivity, but also on the dimensions of the gap of the holder and speed of the wheel and on the volume and type of liquid. The volume transferred per unit area is given by the volume of the liquid used divided by the axial length of the gap and the length of the track achieved.

$$\frac{V}{LB} = K_r + K_a \sqrt{t}$$ [12]

where V is the volume of liquid used (ml),
    L the length of track produced (m),
    B the length of the slot (m),
    T the absorption time (sec.),
    K_r the roughness index (ml/m^2), and
    K_a the absorption coefficient (ml/m^2 √s)

The intercept of the absorption curve K_r is a roughness index and the slope K_a of the curve is an absorption coefficient. The interaction between substrates and a liquid (Papers I and II) was studied using contact angle measurements by a dynamic absorption tester, Fibro DAT (Fibrosystem AB, Stockholm, Sweden). Using this instrument, the wetting, spreading and penetration of droplets was followed by a CCD camera connected to a PC, with a time resolution of 20 milliseconds. The lateral-images (Figure 11) thus obtained were analysed to give the drop contact angle, base diameter, height and volume.
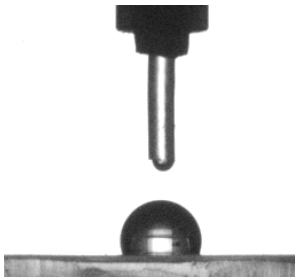

Figure 11. A projection of a droplet of water on a printing plate surface.

An experimental paper web paper testing machine, LINDA (STFI-Packforsk AB, Stockholm, Sweden) was used to study dynamic wetting properties of the substrate in Paper I. LINDA is illustrated with its most important measuring devices in Figure 12, but is described in detail by Blohm and Borg (2001). LINDA can be set up to simulate the transfer of water to a substrate in a printing press. Water can be applied continuously on a moving web in defined amounts. It is possible to measure the change in thickness of the substrate when water is applied. The substrate passes through a pressurized nip, where the compressed thickness is recorded. Changing the speed (14-300 m/min) leads to different times between the water application and the thickness measurement.
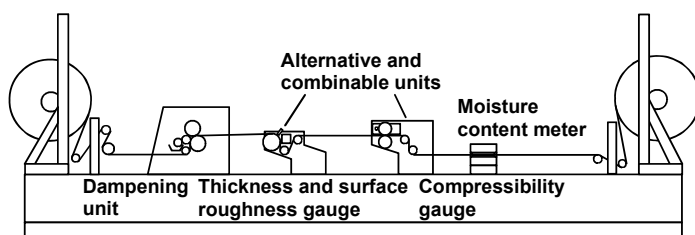

Figure 12. The LINDA machine is used for large-scale dynamic wetting trials. The machine consists of a dampening unit (LAS applicator described in Fellers and Norman 1998) and different gauges. The equipment was used in Paper I.

2.8 Set-up of the flexographic printing press

The printing trials were performed in a CI flexographic printing press, see Figure 3. The diameter of the impression cylinder was 0.9 m and the press had a maximum printing speed of 150 m/min. Print stations and intermediate air dryers surrounded the impression cylinder. The air circulation was always kept on. The air temperature was regulated with a heater.

2.8.1 Water uptake trials

Full-scale water uptake trials were performed in Papers I and II using a six-colour central impression (CI) cylinder press, Figure 13. The printing

33

speed was 50 m/min and some cases at 150 m/min. The printing press is equipped with five inner station air dryers located between each of the six printing units and a final main dryer after the sixth printing unit. The second printing unit was used for the application of water and the model fluids (Table 4) by means of ordinary ink transfer with an enclosed doctor blade chamber, an anilox roll, a plate cylinder with a full-tone layout and an impression cylinder. At the fifth printing unit, water-based ink was transferred by a system similar to that in the second unit, except that the plate cylinder had a chosen layout.
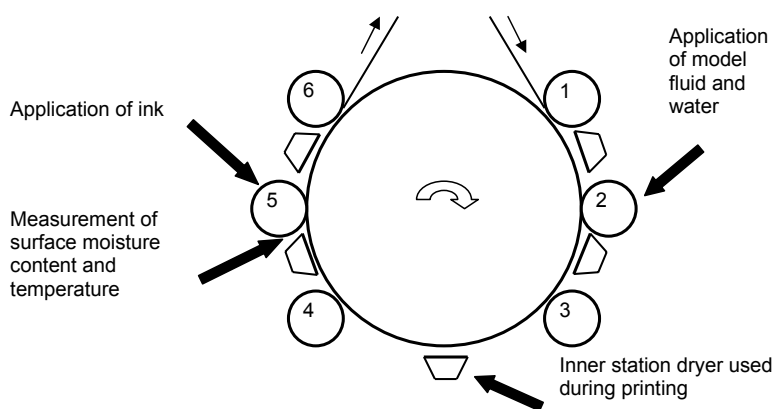

Figure 13. The experimental set-up of the flexographic printing press during the printing trials concerning wetting trials in Papers I and II.

The surface temperature (EL-101, Pentronic, Gunnebo, Sweden) and moisture content (MCA 1410, Fibrosystem AB, Stockholm, Sweden) of the substrate were continuously measured in the printing press with non-contact sensors. The sorption of water and model fluids was also measured gravimetrically. The ink tray was positioned on a scale and the loss in mass of water and model fluids and the numbers of printed metres were registered when the press was running. Model fluids and water were transferred to the substrate by a full-tone plate with a given area.

2.8.2   The dynamic press pulse

An in-situ method was used to measure the dynamic nip pressure in a
flexographic printing press (Paper III). The experimental set-up is described
in Figure 14 and the procedure was as follows; a load cell (FlexiForce,
PIAB Mätsystem AB, Stockholm, Sweden) was attached to a strip and via
conducting glue to an adhesive copper tape which united the strip to a
circuit and the load cell was introduced into the nip between the board
substrate and the printing plate cylinder. As soon as the load cell entered
the nip, data collection started and the strip was detached from the circuit
after passing through the nip. The potential difference at the output of the
circuit depended on the resistance of the load cell. The potential
difference was recorded using an A/D converter (Model Daqbok 260,
Iotech Inc., Cleveland, U.S.A.) and the data were collected at a speed of
2.5 scans per millisecond. Measurements were made on the solid tone area
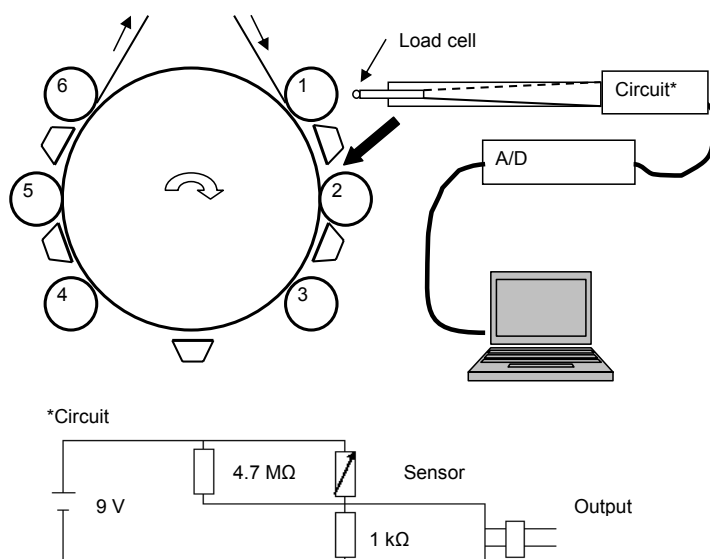of the printing plate.

Figure 14. The measuring technique to determine the dynamic nip pressure in Paper III.

3 Print Quality Evaluation

The evaluation of print results is preferably done on prints printed in a full-scale printing press. A print resulting from one full-scale press is more easily related to another full-scale printing press, because the conditions in such presses are similar. However full-scale printing trials are expensive to implement and laboratory printing presses therefore have an advantage. The printing trials in Paper I-III were done in a full-scale six-colour central impression cylinder press (SoloFlex8480, Windmöller & Hölsher, Germany) Figure 3. The diameter of the impression cylinder was 0.9 metre. The printing press was equipped with five inner station air dryers located between each of the six printing units and a final main dryer after the sixth printing unit.

The IGT-F1 laboratory Flexo Printability tester (Figure 15) can be used at a variety of printing speeds and different impressions. The substrate is attached to a carrier and placed on a rail between the photopolymer printing form and the impression cylinder. When the press is activated, the substrate comes into contact with the impression cylinder and the doctor blade contacts the anilox roll. The nip pressures between anilox roll and substrate and impression roll are set independently. The IGT-F1 Printability Tester (IGT Testing Systems, Amsterdam, NL) was used for the laboratory printing trials in Paper V.

Figure 15. The IGTF1 Printability tester used for laboratory printing in (Paper V). Source www.igt.nl

3.1   Print Density

Print density is an important parameter for every print. Print density is roughly a measurement of how much ink that is transferred to the substrate and its appearance. Too low a print density means that the print looks dull while too high a print density means that half-tone dots tend to fill-in (Johansson et al. 1998). The print density is a measure of the contrast of a print and a logarithmic function is applied in accordance with the general experience that a psycho physiological perception is related to the logarithm of the stimulus. Optical print density, D_V (full tone) and D_R (half-tone) is defined as:

$$D_V = \log\left(\frac{R_\infty}{R_V}\right)$$
[13]

$$D_R = \log\left(\frac{R_\infty}{R_R}\right)$$
[14]

where R_R is the reflectance factor of the half-tones, R_∞ is the reflectivity of the unprinted substrate and R_V is the reflectance factor of the full-tone.

The optical print density D varies from zero to a saturated value, D_∞, Figure 16 as the ink layer on the substrate increases (Tollenaar and Ernst 1961), according to the relationship:

$$D = D_\infty(1 - e^{-mz})$$
[15]

where m represents the slope of the curve $[(dD/D_\infty)/dz]$ in the region of a very thin ink film thickness, z. Havlínová et al (2000) investigated the ink receptivity of paper with offset inks. They applied the Tollenaar- Ernst equation to their experimental data when studying ink mileage for the different papers. The highest D_∞ was achieved with a coated substrate characterized by high values of smoothness, brightness and low penetration.
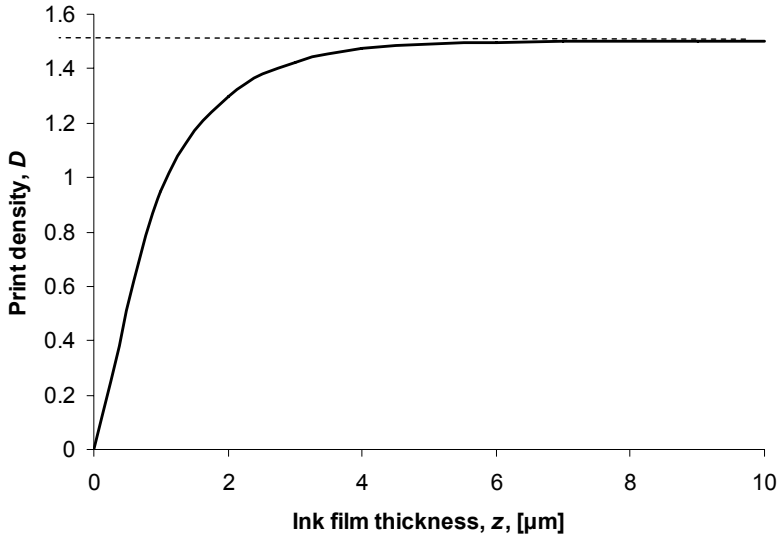
Figure 16. Print density and its relation to with ink film thickness on the paper (m=1 and D_∞=1.5) according to Eqn. [15].

Print density is usually measured by a densitometer in printing houses but it can also be determined with a spectrophotometer. The spectrophotometer measures the reflectance factors in e.g. the 360-740 nm wavelength range with a resolution of 10 nm. Using a spectrophotometer, a specific wavelength can be chosen. At a wavelength 600 nm there is a reflectance minimum corresponding to the absorption maximum in the transmission spectrum of the cyan ink, i.e. this wavelength gives maximum sensitivity for the cyan ink Figure 17.
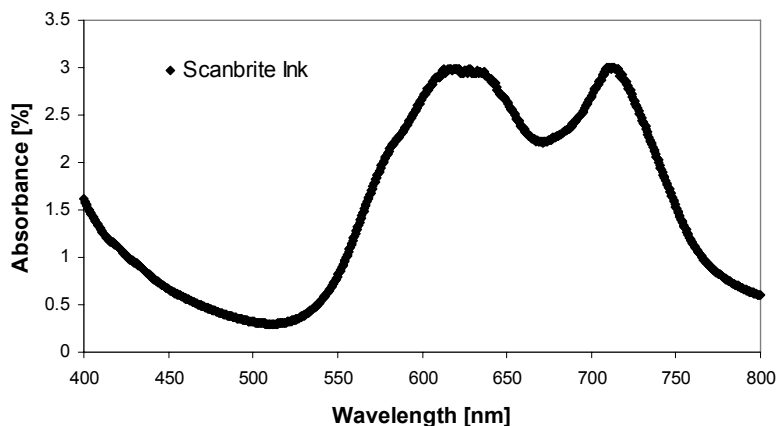
Figure 17. Transmission absorbance spectrum for Scanbrite process cyan.

The "built-in" average reflectance from the mottling software program was used as an indication of print density in Paper I. This was because the measurement aperture of the densitometer is small (3.6 mm) and there were large reflectance variations in the print. The optical print density of the printed samples in Paper II was determined with an L&W Elrepho instrument (Lorentzen & Wettre, Stockholm). The printed samples in Paper III were evaluated with respect to optical print density with a Minolta spectrophotometer CM-3630 (Minolta Svenska AB, Sweden). Optical print density was calculated using Eqns. [13] and [14] in both Papers II and III. The printed samples in Paper V were evaluated with respect to print density with a densitometer GretagSPM100-II (GretagMacbeth, Regensdorf, Switzerland).

3.2   Ink amount on substrate

The amount of ink transferred to a substrate can be estimated by determining the copper content of the printed samples. Printed samples with a known weight are dissolved in concentrated nitric acid in a microwave oven. The copper content can than be determined using Atomic Absorption Spectroscopy at a wavelength of 324.8 nm. The

amount of ink transferred to the substrate was assessed by analyzing the copper content of the printed samples in Papers I and III.

3.3 Dot Gain

Dot gain is a consequence of dot and substrate deformation in the printing nip and a spreading of the ink. The flexographic printing form is compressed in the printing nip and the consequent enlargement of the dot on the plate produces a larger dot. The spreading of ink around a dot in a half-tone area and the deformation of the dot mean that the printed dot becomes larger than the original dot, which the printing process strives to replicate. The combined effect of ink spreading and expansion of the print form is called the "physical dot gain", which is the difference in size between the printed dot and the dot on the plate. In addition the "physical dot gain" there is an "optical dot gain", due to lateral light scattering in the paper (Figure 18). Optical dot gain is always present when print is viewed (perceived or measured) under reflected light.
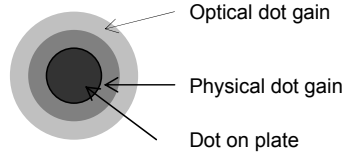

Figure 18. The different components of dot gain.

The total dot gain may be assessed from measurements of the reflectance factor of the half-tone print R in relation to the reflectance factor of the corresponding solid print R_v and the reflectivity of the unprinted paper R_∞. The percentage area A covered by the printed dots is then given by the Murray- Davies equation (Murray 1936):

$$R = AR_V + (1-A)R_\infty \qquad\qquad [16]$$

from which A may be expressed as

$$A = \frac{(R - R_\infty)}{(R_v - R_\infty)} \qquad\qquad [17]$$

Densities of half-tones and full-tone can be calculated according to Eqns. [13] and [14]. The effective coverage of the print, F_D, can be calculated as:

$$F_D[\%] = \left[\frac{(1 - 10^{-D_R})}{(1 - 10^{-D_V})}\right] * 100\% \qquad\qquad [18]$$

where D_R is the halftone density and D_V the solid tone density, and the absolute dot gain in percentage points can be calculated as:

$$Dot\ gain = F_D - F_{nom} \qquad\qquad [19]$$

where F_{nom} is the nominal "tone value" of the negative film. This expression may be valid for the visual dot gain but is not a true representation of the physical dot gain. It gives a value only of the apparent area covered by the dots; the measurement is affected by the optical properties of the paper so that the filling-in appears to be greater than it actually is. For dot gain evaluation in Paper I, the print density was determined with a densitometer (Gretag D19C, X-rite, Regensdorf, Switzerland) with measuring geometry 0°/45°. The Murray-Davies Eqns. [18] and [19], was used to calculate the dot gain. In Paper III, the reflectance values of the half-tones measured with the Minolta spectrophotometer were used to calculate print density and the dot gain according to Murray-Davies. The same procedure was followed for the reflectance values measure by the Elrepho in Paper II. Dot gain in Paper V was calculated with the Murray-Davies equation using the print density values from the GretagSPM-II.

41

3.4   Print Mottle

Print uniformity, mottling, is an expression for the evenness in optical density and print gloss. Figure 19 displays an example of printed matter exhibiting print mottle at two levels. Mottling can be calculated through a Fourier transform analysis of variations in reflectance factor intensities in the x-y plane from images captured by, for example, a calibrated flatbed scanner. The result is often reported as coefficient of variation and variations are reported for the spatial wavelength range of 1-8 mm (Johansson 1999). Blokhuis and Kalff (1976) used a dynamic smoothness tester on paper to predict unevenness in print.
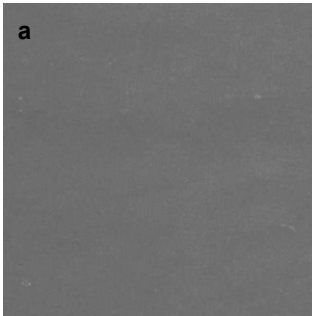
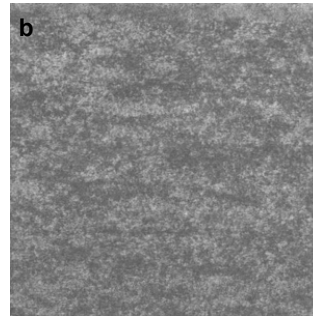Figure 19a. Print mottle= 1.34; Print density= 1.5 and Reflectance factor=23.8%

Figure 19b. Print mottle= 14.20; Print density= 1.0 and Reflectance factor= 28.5%

The dynamic smoothness tester is basically on a combination of existing methods, the IGT printability tester, the Chapman smoothness method and a microdensitometer. They found that the periodicities of the unevenness in the print and the unevenness of the paper were of the same magnitude. Mottling was evaluated using the program STFI-Mottling v2.4 and STFI-Mottling v2.42 (STFI-Packforsk AB, Stockholm, Sweden) for Paper I and II, respectively. The sampled area was 43.3×43.3 mm^2 (sample area for hard printing plate was 21.7×21.7 mm^2). Each sample area (43.3×43.3 mm^2) analysed with respect to mottling was also analysed with regard to average reflectance in Paper I. The sample area was 43.3×43.3 mm^2 in Paper II. The reflectance variations within a spatial wavelength of 1-8 mm were used. A related method for determining loss of ink in e.g. full tone area is UnCovered Areas (abbreviated UCA). The UCA is generally

within the range of 0.04 to 0.9 mm² (Stora Enso Research Falun, Sweden). The full-tone areas were analysed with respect to UnCovered Areas abbreviated UCA, (Stora Enso Research, Falun, Sweden). Images were captured by a CCD camera and analysed with regard to the percentage area not covered by ink. The size of the images was 32×32 mm² and their resolution 100 µm/pixel. The result was reported as percentage uncovered area for non-printed areas in sizes from 0.04 to 0.9 mm² in Paper I.

3.5 Print evaluation using multivariate analysis

With multivariate methods it is possible to investigate the relations between all variables in a single context. The multivariate analysis was used in Paper V to investigate different plate parameters influence on print density. These relationships were displayed in plots. The multivariate analysis PLS (Partial Least Square) is a tool for finding how a matrix with defined variables (X variables-plate parameters) influences a matrix with different response variables (Y variable-print density). In PLS the defined variables are projected into a model describing how the response variables are related to the defined variables. The PLS models find the multidimensional direction in the X matrix that explains the maximum multidimensional variance direction in the Y matrix. The original X variables are combined into weights (w*) and the original Y variables are combined into weights called c (Umetrics 2005).

4 Mechanical properties of the plate, tape and sleeve assembly

The thermoplastic elastomer in the plate is viscoelastic (Mirle and Zettlemoyer 1987), which means that it is resilient, but that it also exhibits viscous behaviour. At an infinitesimal strain or rate of strain, the mechanical behaviour of a viscoelastic material can be illustrated as a combination of one or several springs and dashpots imagined as a piston moving in oil (Ferry 1980). Figure 20 describes the Zener model, which consist of a parallel combination of a spring and a dashpot in series with a second spring (MacPhee 1998).
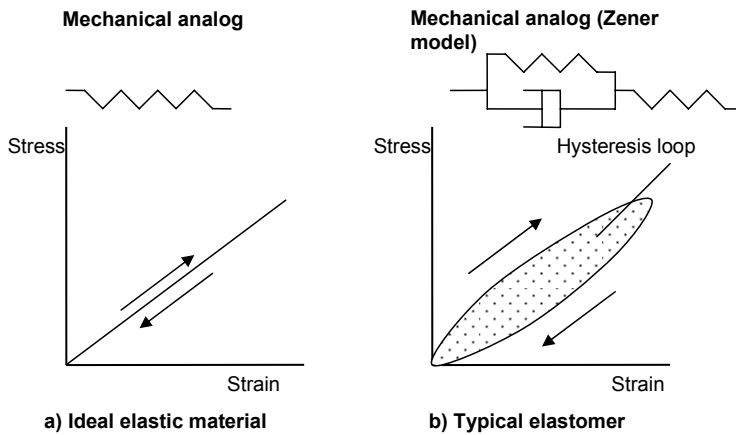

Figure 20. Mechanical models a) ideal elastic and b) elastomer describing mechanical behaviour in the linear elastic range.

The strain is first increased and then decreased at a constant rate of strain. For the elastomer in Figure 20b, the part of the stress-strain curve corresponding to increasing strain lies above the part of the stress-strain curve corresponding to decreasing strain. This is different from the stress-strain curve for an ideal elastic material shown in Figure 20a the two parts coincide. The distance between the parts of the stress-strain curve for the elastomer increases as the rate of strain is increased. If the stress in Figure 20b was changed at an infinitely slow rate, the two curves would coincide and the elastomer would appear as an ideal elastic material and reach the

same maximum stress value as the ideal elastic material. The area between the stress-strain curves in Figure 20b is referred to as the hysteresis loop and is proportional to the amount of heat generated (MacPhee 1998).

4.1.1 Tape and sleeve assembly

The printing plate is mounted directly on the printing cylinder with adhesive foam tape or a compressible cushion sleeve. The advantage of foam tapes and cushion sleeves are their unique compressive behaviour Figure 21. At 1 MPa, the strain for a cushion sleeve is 9 % and less than 1 % for the hard and soft plate. This minimizes the distortion of the dot on the plate when it is in contact with the substrate. The use of a foam layer in flexography is universal in all applications ranging from corrugated post-print to wide web flexible packaging (Kilhenny 2007).
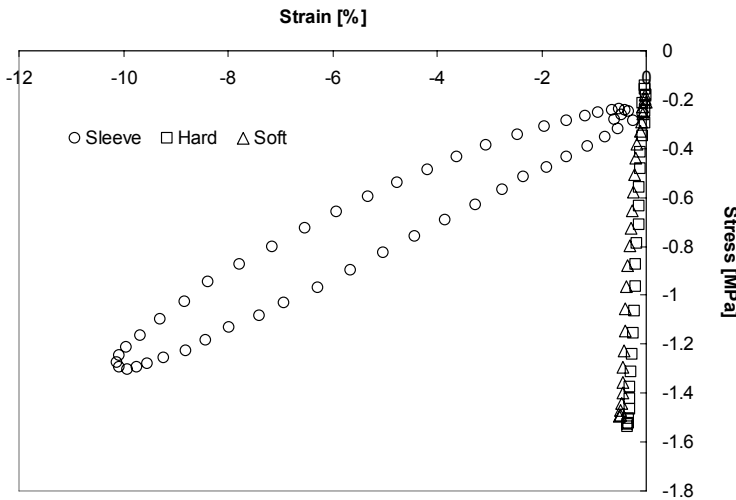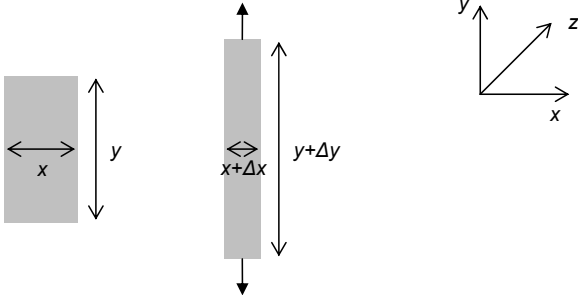

Figure 21. Example of a stress-strain curve for plates (hard and soft) and cushion sleeve (Paper III).

When an elastic material is strained in one direction (y-direction) there is a corresponding negative strain in the x - z plane (Figure 22). The relationship between these strains is called the Poisson's ratio, ν, of the

45

material Eqn. [20]. Poisson's ratio is defined as the ratio between the strain in the transverse, ε_T, and the strain in the longitudinal, ε_L, directions (Nielsen and Landel 1994). This means that the dots or image on the print form are elongated in the print direction. The elongation is uniform for solid tones and for small dots. Two factors determine the image elongation; thickness of the photopolymer layer above the neutral axis, which is displaced to a point just above the polyester bearer, and periphery of the plate cylinder including the plate, tape and mounting matter attaching the plate to the cylinder. The elongation distortion is compensated for in the pre-press process (Anon 1985).

$$\varepsilon_T = \frac{\Delta x}{x}; \; \varepsilon_L = \frac{\Delta y}{y}$$

$$v = \frac{-\varepsilon_T}{\varepsilon_L} \hspace{4cm} [20]$$

Figure 22. The definition of Poisson's ratio

4.1.2 *Influence of over-exposure and weathering tests on plate properties*

The properties of the printing plate are of importance for achieving a good print. Printing is a cyclic process and the plate is subjected to stress from the mechanical action of the rolls. The ink, contains pigment particles and is abrasive.

Sutherland (1982) studied problems arising with photopolymer plates in lithographic printing considering abrasion and wear. She also discussed the polymer composition and printing process, and the wear environment, to reduce the tendency of fatigue wear of the photopolymer.

In Paper V an attempt was made to change the properties of the flexographic printing plate properties by means of over-exposure in the pre-press process (Figure 6) and by means of an accelerated weather tester (Figure 23).

Figure 23. Accelerated weather tester used for changing the properties of printing plates in Paper V.

The properties of the plate were successfully changed as shown by subsequent evaluation of plate properties e.g. roughness, hardness, surface energy and dot shape. An increase UVA-radiation resulted in a higher dispersion of light in the polymer material, and this led to an increased photopolymerization (crosslinking) of the polymer and hardening of the plate, shown in Figure 24. The radiation process may cause a deterioration in the polymer and can form macro-radicals, and chain scission may lead to a decreased molecular weight, or cross-linking may occur which increases the stiffness of the material, as shown in Figure 24 and Table 14 (Seymour and Carraher 1992). The increase in oxidised carbon compared to that of the normally exposed sample for the degraded samples 4h340 and 2cy340 revealed by ESCA analysis in Tables 10 and 11 also indicated a lower flexibility of the polymer (Rodgers and Waddell 2005). The tendency for the dot area to decrease due to degradation (Table 16) could

be an effect of surrounding oxygen together with UVA-radiation and might be a cause of the inhibition effect proposed by Kannurpatti and Taylor (2001). This inhibition effect is to a certain extent favourable because it leads to smaller and sharper dots.
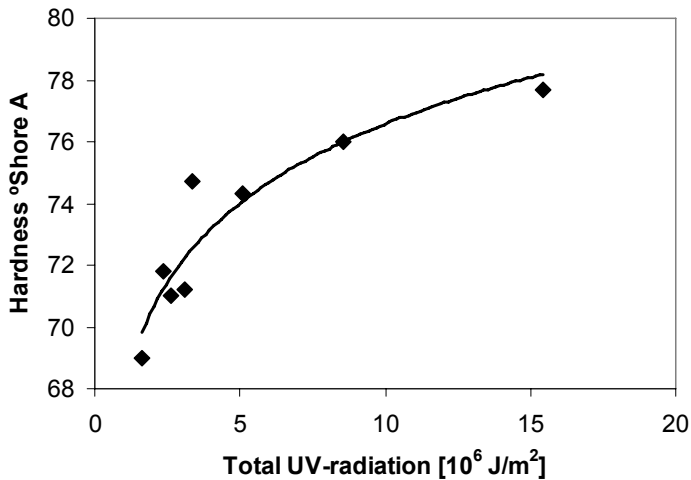

Figure 24. The hardness as °Shore A as a function of the total UV-radiant energy (UVA and UVC) to which the plate was normally exposed, degraded and over-exposed printing

Excessive UVA-radiation may eventually lead to a hard and brittle material with little toughness (Seymour and Carraher 1992). This could cause microcutting of the plate and dot cone-structure i.e. the dot becomes smaller (Sutherland 1982). The tendency for the dot area to increase for over-exposed plates compared to the normally exposed dot could be explained by the prolonged main exposure for 2UVA (Liu et al. 2002), in which case the UV radiation is distributed to a greater extent within the polymer bulk leading to an increased cross-linking, since the polymerization proceeds until the radiation is turned of. The dot shoulder angle (Table 15) was influence most by the over-exposure treatment and when the main exposure was doubled (2UVA) for the 20 % dot, the shoulder angle was increased by almost 3 per cent. This indicated that the time for main exposure partly determines the shoulder angle.

In a parallel study, the polymer degradation of the photopolymer was studied by means of DSC and SEM (Andersson et al. 2008). The study provided insight into important degradation processes of photopolymer printing plates. The knowledge can be used to predict the lifetime of printing plates and to understand the effects of their ageing upon print quality.

4.2   Roller contact and deformation of the cylinder covering

The flexographic printing press, in its most elementary form, is simply an assembly of a rigid roll and a roll with a compliant layer running in contact with each other. The fundamental theory of contact mechanism for frictionless elastic half spaces in contact Figure 25, described by Hertz is simple but powerful, Eqns. [21]-[23] (Johnson 1985). Approximate values of the nip length $2a$, peak pressure p_0 and pressure distribution $p(x)$ can be obtained.

$$E* = \left(\frac{1-v_1^2}{E_1} + \frac{1-v_2^2}{E_2}\right)^{-1} ; \ R = \left(\frac{1}{R_1} + \frac{1}{R_2}\right)^{-1} ; \ -a \leq x \leq a$$

$$a = \left(\frac{4PR}{\pi E*}\right)^{\frac{1}{2}} \qquad\qquad [21]$$

$$p_0 = \left(\frac{PE*}{\pi R}\right)^{\frac{1}{2}} \qquad\qquad [22]$$

$$p(x) = \frac{2P}{\pi a^2}\left(a^2 - x^2\right)^{\frac{1}{2}} \qquad\qquad [23]$$

where P is the applied line load, E_1 and E_2 the elastic moduli of the rolls, v_1 and v_2 the Poisson's ratios of the rolls and R_1 and R_2 the radii of the rolls. A given force applied to a more compliant printing plate will yield a longer nip length than the same force applied to a less compliant printing plate. However the validity of the results given by Hertz is a matter for

discussion considering the assumptions made in the theory, since the Hertz theory does not take into account layered structures.

In Paper IV, a correction procedure taking into account the size of the load cell, used in Paper III, was developed in order to estimate the maximum dynamic pressure in the printing nip. The pressure profile was assumed to follow a cosine relationship. This assumption was made on the basis of the raw data acquired from the sensor.
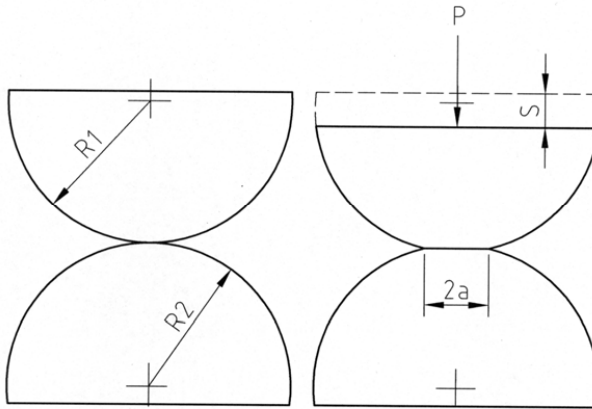

Figure 25. Impression of two rollers.

Deshpande (1978) used a "non Hertzian" contact model to calculate the nip width and showed that the nip width was approximately proportional to the cube root of the applied force.

Hannah (1951) considered disk-shaped rollers in contact, where one roller had a steel core and a thin compliant elastic layer and the other was made of steel. Hannah investigated mathematically the contact length and pressure distribution between the rollers and concluded that the layer thickness, elastic modulus and roller diameter were the most important factors determining the relation between these rollers. High pressure was necessary to establish the same contact length for a thinner elastic layer, but the pressure distribution over the contact zone was only slightly affected by the layer thickness.

Miller and Poulter (1961) used a printing apparatus (PATRA) to measure the nip length of different cylinder coverings. They declared that cylinder coverings should contain a combination of compressible and incompressible layers and should be thick and relatively hard rather than thin and soft.

Keller (1991) used force transducers embedded in a metal roll to measure the nip pressure and time profiles in a calender nip for different roll temperatures, nip loads and speeds. He also investigated the effect of pressure on paper properties and showed that paper compression is more impulse-related than pressure-related at high temperatures, probably due the softening effect on paper fibers.

Bould et al. (2004) used a numerical model to investigate the dot deformation behavior through the printing nip. The deformations of the dot were due to two mechanisms; first an expansion of the dot surface and second a barreling of the dot shoulder. The barreling effect seemed to be the dominant one. Bould et al. (2007) determined the anilox roll-plate contact with a numerical model for a flexographic printing plate. The model described how half-tone dots were deformed in the printing nip when the location of the anilox roll cells relative to the half-tone dot on the plate was varied. They found that the deformation of the dot into the cell was greatest when the centre of the anilox roll cell was directly above the edge of the dot top surface. Numerical modelling experiments have been performed by Lim et al. (1996) to describe the appearance of the pressure pulse in the nip. Their non-newtonian model to predict the elastohydrodynamic behavior in a soft rolling contact gave results which agreed well with experimental data.

In Paper III, the dynamic pressure pulse was measured in a flexographic CI-printing press by means of thin load cells. It was shown that an increased impression led to a higher dynamic nip pressure but neither printing speed nor plate material ("soft" or "hard") had any significant influence on the maximum dynamic nip pressure. Figure 26 shows the maximum pressure and dwell time as a function of press speed for the "soft" and "hard" printing plates. The dwell time decreased and the nip length increased with increasing web speed. The "soft" printing plate

showed a clear relationship between impression and pressure. The "hard" printing plate showed a similar behavior, but it was less pronounced when the impression increased from 200 to 300 µm.

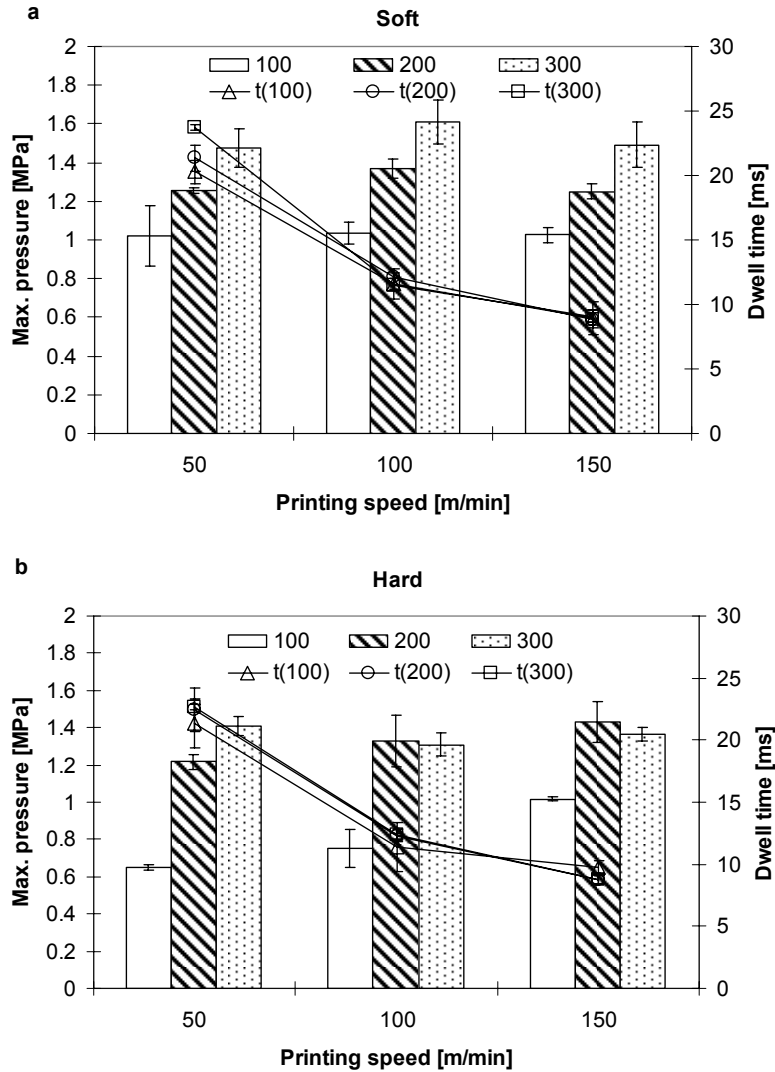Figure 26. Maximum pressure, columns left-hand y-axis, and dwell time, lines right-hand y-axis, for a)"soft" and b)"hard" printing plate at different printing speeds (50, 100 and 150 m/min) and different impressions (100, 200 and 300 µm). Error bars indicate standard deviations. Graphs taken from Paper III.

5   Ink transfer

The amount of ink transferred to the substrate in flexo controlled primarily by the anilox roll's cell volume and cell count (Bould et al. 2007), but it also depends on the printing conditions, substrate and ink properties.

The classical view of the printing process (Walker and Fetsko 1955) can be described as follows. A printing plate covered with ink comes into contact with the substrate in the printing nip. The ink wets the substrate and adheres to it. A fraction of ink is absorbed or immobilized in the substrate (absorbent) in the printing nip. The free ink film, non-immobilized ink, splits between the printing plate and the substrate at the nip exit. Walker and Fetsko also derived ink transfer curves for paper. The amount of transferred ink, y, on coated paper when using a high ink film thickness was expressed as:

$$y = b + f(x - b) \qquad\qquad [24]$$

where b is the acceptance or immobilization capacity of the paper surface for the ink during impression, f the fraction of the free film transferred to the paper and x the amount of ink on the plate before impression. The ink transfer curve in its complete form is more complex and can be written as:

$$y = \left(1 - e^{-kx}\right)\left[b\left(1 - e^{\frac{-x}{b}}\right)(1 - f) + fx\right] \qquad\qquad [25]$$

where k is a constant. Walker (1981) showed that the simplified linear form Eqn. [24] is only a first approximation solution that is generally fairly good for coated paper but that it can introduce serious errors when used on uncoated paper. Walker suggested other methods for determining the transfer constants that give a better fit to experimental data. A more recent modification of the ink-transfer equation was proposed by Zang (1993), who introduced a splitting function F.

$$F = f_\infty + \left(0.5 - f_\infty\right)e^{-2f_\infty x} \qquad\qquad [26]$$

and the modified equation was:

$$y = \left(1-e^{-kx}\right)\left(b\left(1-e^{-\frac{x}{b}}\right) + \left\{\left[f_\infty + (0.5 - f_\infty)e^{-cf_\infty x}\right]\left[(x-b)\left(1-e^{-\frac{x}{b}}\right)\right]\right\}\right) \quad [27]$$

where f_∞ is the splitting factor at high ink levels, and q and m are constants that describe the rate at which the splitting function reaches the value f_∞. Other studies have attempted to link parameters of the Walker-Fetsko equation to physical and chemical properties of the ink, substrate and printing conditions (Karttunen 1973 and Mangin et al. 1981).

In the printing nip between substrate and printing plate, the ink film is exposed to pressure, temperature and shear-rate gradients. Since the ink viscosity is influenced by temperature and shear-rate, these gradients lead to confined regions of reduced viscosity, which control the point of film split (Taylor and Zettlemoyer 1958). Taylor and Zettlemoyer concluded that the position of the ink split in the free ink film was closer to the substrate than to the plate, and that it varied with ink properties and substrate properties. However, De Grâce and Mangin (1986) did not agree that asymmetric splitting ($f < 0.5$) was controlled by a temperature gradient at the liquid/substrate interface. Nor could they confirm that regions of shear thinning in the ink could be an explanation of asymmetric ink film splitting. Their explanation was that "surface asperities" and air entrainment control asymmetric splitting. The properties of the substrate surface and of the printing form play an important role in ink transfer in combination with factors such as speed and nip pressure.

5.1   Effects of press conditions on ink transfer

Frøslev-Nielsen (1962), Schaeffer et al. (1963), Hsu (1962), Cozzens et al. (1967), Walker and Fetsko 1955, Mangin et al. 1981, and De Grâce and Mangin (1984) have all shown that a decrease in printing speed and an increase in the impression pressure increase the total ink transfer to the substrate.

Paper III it was also showed that ink transfer increased with increasing impression (pressure) and decreased with increasing printing speed (dwell time), Figure 27. The experimental set-up is described in Figure 14. In addition the ink transfer differed between a soft plate and a hard plate even though it was concluded that the main deformation occurred in the sleeve, according to the graph shown in Figure 20. This was explained by a complying effect of the soft plate, which follows the irregularities of the rough surface better than the hard one. This led to a higher contact area between the plate and the substrate and a greater ink transfer.
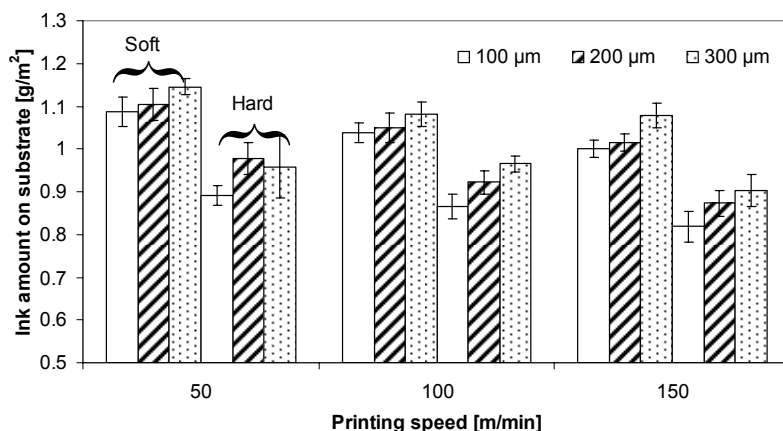

Figure 27. Dry ink amount on substrate using "soft" and "hard" solid tone printing plate at different printing speeds (50, 100 and 150 m/min) and at different impressions (100, 200 and 300 µm). Error bars indicate standard deviations. Graph taken from Paper III.

Schaeffer et al. (1963) made proof press studies of the transfer parameters b and f and how they varied with pressure and printing speed. Among other things, they concluded that b decreased with decreasing printing speed, which was explained by an increase in the extent of paper compression and a decrease in effective capillary diameters. They also concluded that f increased with decreasing printing speed. This was explained by the prolonged and more extensive decompression of the paper, which promotes a greater capillary flow of the increased fraction of ink transferred. Hsu (1962) also declared that with a higher ink viscosity the influence of printing speed and pressure was less.

55

Bohan et al. (2003) evaluated the impact of nip pressures between ink-chamber-anilox roll, anilox roll-plate and plate-central impression cylinder on print density in half-tones and solid tones, and they found that print density was significantly affected by the anilox roll to ink chamber pressure. When this increased, the printed ink density also increased. The plate to central impression nip pressure mainly influenced the printed dot gain.

5.2   Effect of substrate properties on ink transfer

The characteristic properties of printing paper are, according to Parker (1976), its absorbency, permeability, reflectance, opacity, compressibility and roughness. These properties are to some extent related to its porous morphology. There are additional properties of paper such as gloss, surface strength and dimensional stability which also affect print quality. Zang and Aspler (1995) concluded that surface roughness, porosity, and water absorbency are the most important features of the substrate when printing on linerboards with water-borne inks.

5.2.1   Surface roughness and compressibility

Roughness is a measure of the topographic relief of the surface. Roughness can be determined directly from surface-profile measurements, or it can be calculated from light scattering measurements using a theory relating scattering to surface roughness (Bennet and Mattsson 1999). The arithmetic mean deviation of the surface area or profile, *Ra*, describes roughness.

Arney et al. (1994) measured the topographic variations of a surface using the goniometric reflection of light. Their technique determined the topographic gradient, tan (α), and the topographic height is calculated by numerical integration of the gradient across the lateral dimensions of the sample.

Hansson and Johansson (1999) developed a method for the simultaneous measurement of surface topography and ink distribution on prints. The method is useful for predicting the print result with a given surface topography. Some of the applications of the method are specified in Hansson and Johansson (2000).

The roughness of the substrate surface is dependent on and is changed by the pressure applied in the printing nip (Bristow, 1982). The surface compressibility is thus as an important property for the printer. In Paper I, the print simulation was performed in the LINDA equipment Figure 12. Figure 28 displays the thickness change when a mechanical load is applied to the running web at different levels of water application.
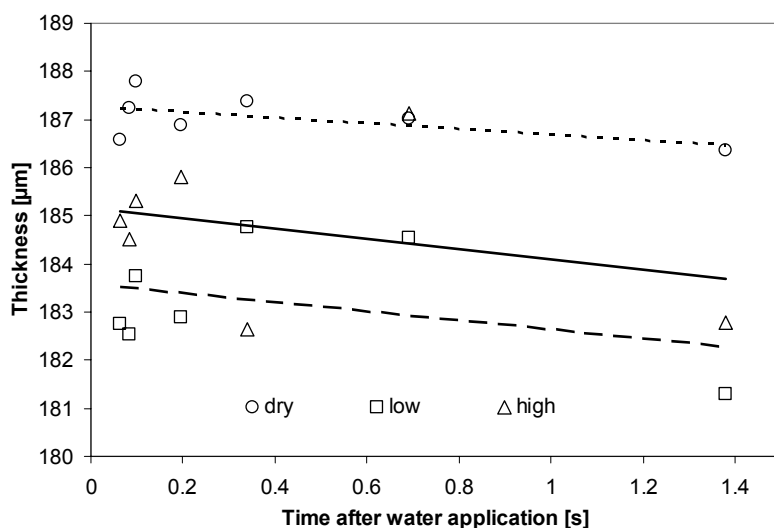

Figure 28. Compressed thickness at a pressure of 0.4 MPa as a function of time after different levels of water application for WTL. Dotted line represents no water application, dashed line represents low (1 g/m^2) water application and solid line represents high (2 g/m^2) water application. (Graph taken from Paper I).

The investigated substrate was WTL (White Top Liner). The water was applied 0.32 m from the load. Low and high levels of water corresponded to water transfers of 1 g/m^2 and 2 g/m^2, respectively. When a pressure (0.4 MPa) was applied, the thickness of the substrate decreased with increasing

amount of water applied to the running web. No significant difference between high and low water application was detected, see Figure 28. Water application led to an increase in surface compressibility (thickness decrease), thus a higher contact area with the printing plate was possible. Similar effects of applied water on compressibility were observed even when a lower pressure of 0.1 MPa was applied.

The thickness of the ink film on the printing plate necessary to achieve contact and transfer and to cover the fiber surface depends on the topography of the paper surface (Mangin and Geoffroy 1989). They defined a term "printing roughness" as the roughness of the substrate in contact with the ink during compression. They concluded that printing roughness was linearly related to the logarithm of the printing pressure. The slope of the regression line yielded a compressibility parameter K', which was a function of both paper structure and nip dwell time. Mangin (1986) concluded that the PPS compressibility ratio is not suitable as a measure of the surface compressibility of coated paper, but their proposed model showed that the absolute compression of the coatings increased linearly with the coating weight.

Ullman and Qvarnström (1976) investigated the print unevenness in full-tone areas of newsprint grades. They concluded that the surface roughness of the substrate predominately controlled the print unevenness.

5.2.2 Porosity

De Grâce and Mangin (1984) have shown that a more porous substrate allows a significantly larger amount of ink to be hydraulically impressed during printing than a non-porous substrate at the same level of roughness. They also showed that the point of maximum fractional transfer (maximum y/x) increased with increasing roughness and porosity at a high initial ink film thickness on the printing plate.

Hsu (1962) studied the flow of ink into a paper structure. He found that at least three factors controlled the flow of ink for a given paper-ink system, namely ink film thickness, printing speed and printing pressure. Hsu also

concluded that a higher ink viscosity led to a lower degree of penetration of the ink into the substrate, although the penetration was also dependent on the porosity of the substrate. An increase in the amount of ink on the printing plate led to an increase in ink penetration into the substrate, but only to a certain level since the substrate became saturated with ink. A very porous paper, antique book paper, did not reach the saturation level at all (Hsu 1962).

A simple estimation using the Poiseuilles equation and Lucas-Washburn equation were performed in Paper I in order to compare the possible driving forces of capillary and pressurized penetration. The Lucas-Washburn equation can only explain the driving force for penetration if the contact angle is less than 90°. This was only the case with SSE and AD applied on WTL. The penetration of liquid into the substrate in the case of water and APG on WTL could only be explained in terms of pressure driven penetration (i.e. the Poiseuille's equation) or by a diffusion mechanism. The time available for pressurized dewatering according to Poiseuille's in Paper I is equal to the nip length divided by the speed. The nip length was measured to be 10 mm by means of a 0.1 mm thick pressure sensor. A web speed of 50 m/min corresponded to a residence time in the printing nip for 12 msec. and the static nip pressure was 0.4 MPa (measure by the same type of pressure sensor). The time for capillary driven dewatering according to Lucas-Washburn was at a web speed of 50 m/min equal to 0.86 sec.. The contact angle between WTL and the fluids applied in the second printing nip was higher than 90°, except for the solutions of AD and SSE where the static contact angle was 52° and 48°, respectively. Insertion of estimated times for pressure driven flow (12 msec.), capillary driven flow (0.86 sec.) and pore radius for WTL from Table 2 in Eqns. [10] and [11] gave a possible uptake from each process of much greater magnitude than the applied moisture levels as given in Table 17. The porosity (Eqn. [9]) of WTL was 34 % according to mercury intrusion experiments, which implied that an uptake of 1.8 g moisture per m^2 corresponds to an average penetration depth of 5.3 µm. Eqn. [10] gave a penetration depth of 1.6 mm (assuming ΔP=0.4 MPa during the entire contact time) and Eqn. [11] gave a penetration dept of 3.5 mm (AD) and

3.7 mm (SSE). This indicates that no film of liquid water existed on the surface when the web entered the fifth printing nip.

5.3   Surface tension, wetting, spreading and ink transfer

Surface tension can be explained by two processes, cohesion and adhesion (Hiemenz 1977). Figure 29 shows columns of liquid of unit cross section representing the processes. Each of these is a volume element in an infinite volume of liquid. The work, W_{AA}, needed to pull a column of liquid A apart is a measure of the attraction between two molecules of the two portions.

$$\Delta G = 2\gamma_A = W_{AA} \qquad [28]$$

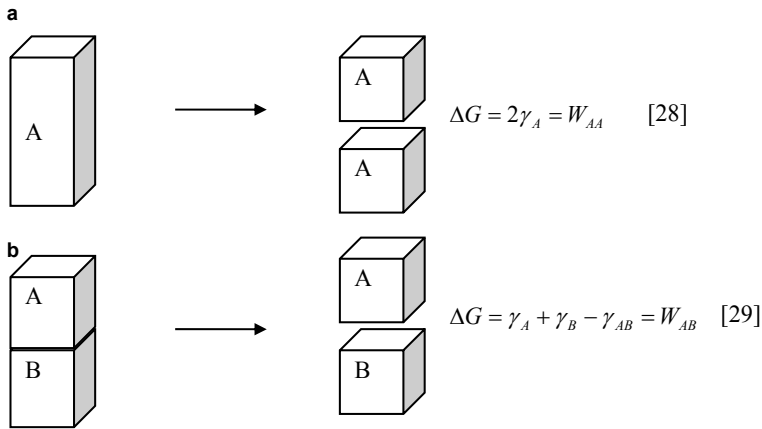$$\Delta G = \gamma_A + \gamma_B - \gamma_{AB} = W_{AB} \quad [29]$$

Figure 29. Schematic pictures of processes for which ΔG equals a) Work of cohesion and b) Work of adhesion.

The separation process for two immiscible liquids A and B is shown in Figure 29b, where the work, W_{AB}, is a measure of the adhesion between two different phases. The difference between the work of adhesion and cohesion of two substances defines a quantity known as the spreading coefficient of B on A, $S_{B/A}$

$$S_{B/A} = W_{AB} - W_{BB} = \gamma_A - \left(\gamma_B + \gamma_{AB}\right) \qquad [30]$$

When $W_{AB} > W_{BB}$, the interaction between A and B is sufficient to support the wetting of A by B. A positive spreading coefficient means that B will spread on A spontaneously. In essence, a liquid will spread spontaneously only on a solid that has a higher surface energy than that of the liquid.

A droplet of water may spread out over a surface or retain its drop-like profile. This depends on the chemical character and structure of the surface. If the surface is of a polar nature, the dipole molecules of the water tend to spread out on the surface and there is an attraction between the surface and water dipole molecules and the contact angle is low. If the surface has a non-polar surface and lacks attractive forces, the water droplet does not favour contact with the surface and it therefore forms as small contact area as possible, which gives rise to a large contact angle.

5.3.1 Wetting and spreading and implications for ink transfer

In water-borne flexographic printing, the surface energy of the liner board is important. The wetting of a paper surface by the ink is one of the basic requirements for ink absorption and ink transfer (Zang and Aspler 1995). The surface tension of flexographic water-borne ink ranges from 20 to 40 mJ/m^2 (Micale et al. 1989), and, in order to achieve good print quality, the surface energy of the linerboard surface must be higher than that of the water-borne ink.

Sheng et al. (1999) reported that surface energetic of linerboard influenced the print density. Unsized papers had a higher surface energy than sized papers, thus unsized papers were more ink-receptive than sized papers.

The mass transfer of fluids in the full-scale printing trials in Paper I showed that the transferred amounts were different for different substrates and liquids (Table 17). The nominal ink capacities for the anilox rolls are stated in Table 5.

Table 17. Uptake of 0.3 wt.-% APG, 1 wt.-% SSE and ink (g/m^2) by substrate in the CI-press using a full-tone printing layout and two different anilox rolls. The nominal ink capacity for 120 l/cm and 195 l/cm is 8 and 4 g/m^2, respectively.

Substrate	Moisture uptake [g/m^2]				Ink uptake [g/m^2]
	Anilox 195 l/cm		Anilox 120 l/cm		Anilox 120 l/cm
	0.3 wt.-% APG	1 wt.-% SSE	0.3 wt.-% APG	1 wt.-% SSE	
WTL	0.7	0.9	1.8	1.8	2.3
A	0.5	0.8	1.3	1.5	2.3
B	0.6	0.9	1.4	1.5	2.2

Transfer ratios calculated from these measurements, roughly confirm "the rule of thumb" that some 50% of the liquid is transferred in the nips (anilox roll-to-printing plate-to-substrate) (Walker and Fetsko 1955 and Kipphan 2001). There are however, some interesting deviations from that behaviour for both substrate and liquid. The transfer ratio for the ink differed from the ratio for the model fluids (0.3 wt.-% APG and 1 wt.-% SSE), and the different substrates gave different transfer ratios, at least when the anilox roll 120 lines/cm was used. It is not surprising to find variations in transferred amounts, since the surface energy and viscosity differ for the liquids, and the surface energy, roughness, formation and porosity differs for the substrates and it is known that these properties affect ink transfer (Darhuber, 2001, De Grace 1983, Frøslev-Nielsen, 1962 and Havlínová 2000).

The water-borne ink consists of at least 50 %, by weight, of water (Laden and Fingerman, 1997), so that the substrate is exposed to water during printing, and this can affect its properties. The water interacts with fibers and the fiber network. The penetration of aqueous liquids into the paper is further complicated by absorption into fiber walls and this increases the fiber wall thickness, because aqueous liquids break and replace interchain hydrogen bonds in cellulose (Lyne, 2002). It has been reported that fibre rising and sheet roughening result from the interaction of water with fibres and with fibrous flocs on the paper surface. These phenomena may be seen in processes like coating and printing where water is applied to the paper (Aspler, 1994). The water-induced roughening is related to changes

in the cross-sectional shape of the fibres. The most thick-walled fibres have the largest lumen opening even after calendering, and they thus make the greatest contribution to the surface roughening (Forseth et al. 1996). The roughening of a substrate by moisture is due more to bulk changes than to surface effects (Toshiharu and Lepoutre, 1999). They argued that the bulk structural changes occur as a result of water molecules diffusing into the fiber wall causing e. g. a volumetric expansion in the cross-section leading to a plasticization of the hemicellulose which releases both shrinkage and calendering-induced stresses which strive to keep the fiber cross-section collapsed.

Åslund (2004) used an optical method to measure water-induced roughening of paper surfaces and noticed that for substrates containing mechanical pulp there was an almost linear relationship between the relative change in surface roughness and the amount of water transferred. In printing, the absorption properties of a paper are of fundamental importance for the runnability of the press.

In Paper I and II the Bristow absorption tester was used to evaluate the interaction of water and surfactant solution with different substrates. Bristow 1967 came to the conclusion that wetting is divided into two steps; first an initial wetting (at least for water) including the transfer of the liquid to the substrate and then a second step; involving the rearrangement and absorption of the liquid on the substrate. An example of the absorption curves for substrates are given in Figure 30.
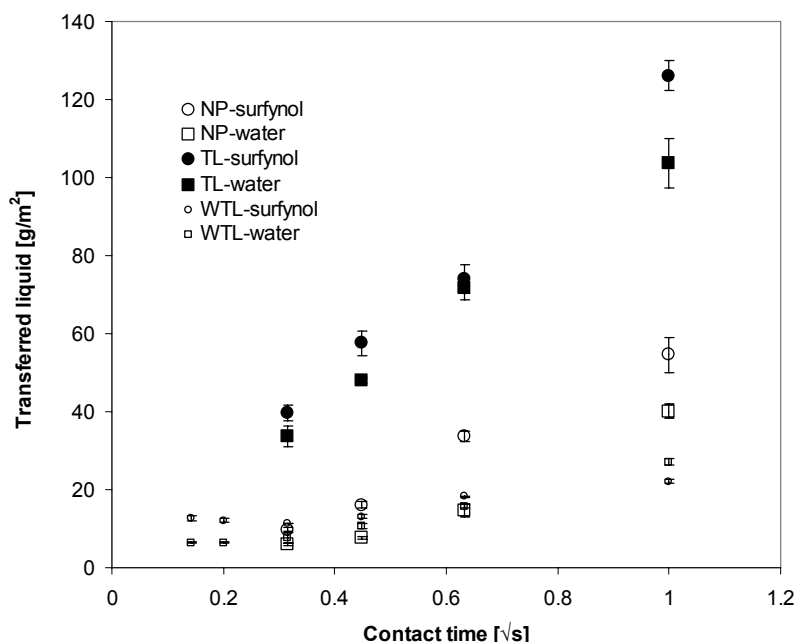
Figure 30. Transferred liquid, water and surfactant solution (0.1 wt.-%) on NP, TL and WTL at 23˚ and 50% RH as a function of the square root of time. In the case WTL-water and WTL-surfynol there is an initial wetting time before absorption occurs. Figure from Paper II.

The white top testliner (TL) shows a considerable uptake of both surfactant solution and water. Newsprint (NP) shows a slower uptake of liquids than TL. Water on NP shows the least spreading and the lowest absorption. At a contact time of one second, water uptake by NP and TL is 40 g/m² and 105 g/m², respectively. The uptake by white top liner (WTL) is lower and slower than by NP. A water uptake of 27 g/m² at one second is reported. The data obtained using the FibroDAT equipment for the interaction between the substrates and water and surfactant solutions in Papers I and II are shown in Figure 31a, where the volume of the drop is plotted as a function of time, a steep negative slope indicating a fast absorption. The fastest absorption was obtained for the surfynol solution on TL, whereas only a slow absorption was observed for water on NP. On both substrates, the surfynol solution was absorbed more rapidly than water, and both liquids were absorbed more rapidly by TL than by NP.

Data for WTL are taken from Paper I and Figure 31a shows that there was no absorption of the liquids on WTL.
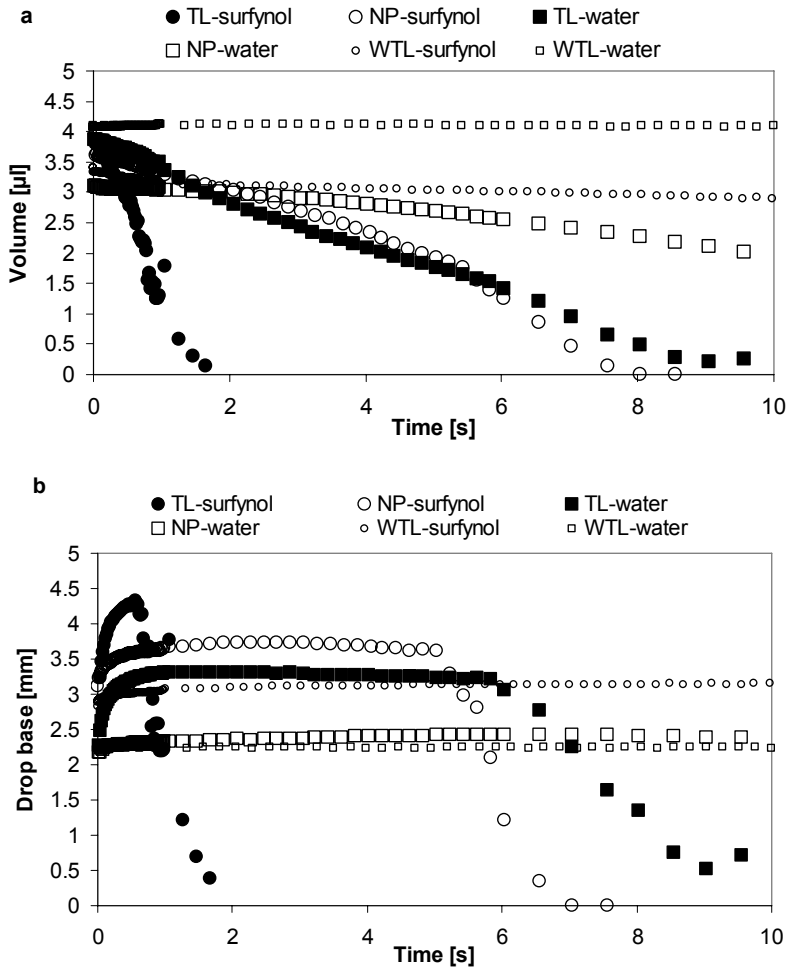

Figure 31. a) Interaction between liquids and substrate using Fibrodat. a) The volume of a drop of liquid on NP (Newsprint), TL (white test liner) and WTL (white top liner) versus time at 23° and 50% RH. b) The base diameter of a drop of liquid on NP, TL and WTL versus time at 23° and 50% RH. (Paper II).

Figure 31b shows the base diameter of the liquid drop versus time, displaying three fairly distinct events. First, there is an initial rapid

spreading of the drop as the diameter increases. Second, the drop diameter remains constant while liquid is absorbed and, third, the diameter decreases as the drop finally disappears. On NP, the diameter of the surfactant drop was 3.1 mm, whereas that of the water was 2.2 mm. With both liquids, spreading was faster on TL. The surfactant spread and was absorbed by the TL within two seconds, whereas the absorption of water by TL, occurred after approximately 6 seconds. Figure 31b also includes the base diameter behaviour on WTL. A small initial spreading was seen for the surfactant solution, but no significant absorption of the liquids was observed.

Trollsås (1995) studied the water uptake of newsprint in a full-scale offset production printing test, at printing speeds of 132 m/min, 264 m/min and 372 m/min. The test showed that the water uptake was approximately 0.5 g/m^2 per printing nip on each side of the paper. He also noticed a tendency for to decrease with increasing substrate roughness. In Paper II the water up-take of newsprint in a flexographic CI-printing press was studied (Figure 3) and the experimental set-up of the press is shown in Figure 13. The water uptake on one side at printing speeds of 50 m/min and 100 m/min were 1.2 g/m^2 and 1.3 g/m^2, respectively at low application and 2.4 g/m^2 and 2.4, respectively at high application.

Aspler et al. (1984a) investigated the phenomenon of self-sizing of newsprint, and came to the conclusion that, after self-sizing has occurred, surfactant addition can restore the wettability of newsprint and its sorption of water. A more recent study by Aspler et al. (2004) showed that changes in wettability (measured as contact angle) of internally sized solid bleached linerboard had no effect on the transfer and holdout of water-borne flexographic ink. In Paper II, on the other hand, it was shown that the UCA in full-tone areas on a surface-sized white top liner (WTL) was affected by moisture application in a previous printing unit. The UCA was reduced by "pre-printing" with a surfactant solution. The same tendency was observed when a large amount (~2 g/m^2) of water was transferred, Figure 32.
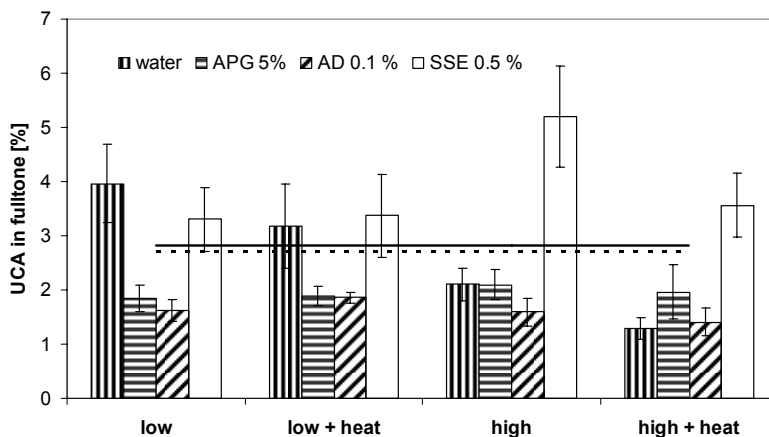
Figure 32. UCA (0.04-0.9 mm^2) in fulltone areas for WTL at different levels of water or model fluid application (low and high) and two levels of heat (no heat 0 kW and heat 10 kW). Solid line represents no application of water or surfactant solution but with heat supply. Dashed line represents no application of fluid or heat. The soft printing plate was used. Error bars indicate standard deviation.

Aspler et al. (1993) investigated the setting of water-borne inks and print quality on uncoated paper and how they were influenced by pH (of the paper surface) and water absorbency. They found that ink transfer increased with increasing water absorbency (less sized papers) and that the pH had only a small effect on ink transfer. Although the dwell time in the nip was short (~1 ms), there was sufficient time for surface chemistry to play a role.

6 Summaries of Papers

6.1 Paper I: The interaction between water and paperboard and liner in a flexographic printing press

In this study, the consequences for the print quality of a pre-treatment of the surface by water and heat were studied in a full-scale central impression (CI) flexographic printing press. The experimental set-up (*Figure 13*) was chosen in order to mimic the effects of aqueous ink applied in a former printing units and subsequent air-drying units. The substrate properties are summarized in *Table 2*. the properties of the used inks in *Table 3*, the model fluids in *Table 4* and the anilox rolls, plates, tape and sleeves used in *Tables 5* and *6*. The printing conditions are shown in Table 18.

Table 18. Surface temperature (T) and moisture (M) content for WTL with different applied model fluids and water at printing trials with the air heater turned off or at 10 kW. The anilox rolls with low and high ink capacity are denoted as low and high, respectively. Data for T and M without applied fluid in print unit two are included. Surface temperature and moisture for the dry case at 0 kW was 19.0 °C and 5.5 %, respectively and at 10 kW 22.0°C and 5.3 %, respectively.

Fluid	0 kW/low		10 kW/low		0 kW/high		10 kW/high	
	T [°C]	M [%]	T [°C]	M [%]	T [°C]	M [%]	T [°C]	M [%]
Water	17.7	5.6	20.0	5.6	18.8	6.3	20.5	6.2
APG 5%	20.1	5.8	21.1	5.7	19.3	6.7	20.9	6.6
AD 0.1%	18.8	5.8	20.5	5.7	18.9	6.4	20.6	6.5
SSE 0.5%	19.2	6.0	20.8	6.0	19.4	6.3	20.1	6.5

The surfactants were added to promote sorption on the uncoated substrate and in order to ensure that printing in the later printing unit was not performed on top of a water film. The estimate using the Poiseuille equation [10] and the Lucas-Washburn equation [11] showed that no film of liquid water existed on the surface when the web entered the fifth printing nip.
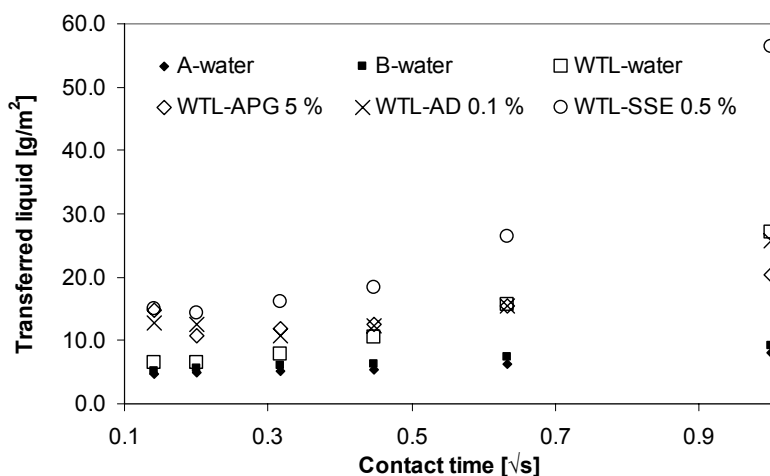
Figure 33. Amount of fluid transferred to substrate A, B and WTL as a function of contact time using the absorption tester. Transferred fluids are water, surfactant solutions (APG 5% and AD 0.1%) and SSE 0.5%.

The papers and model fluids interaction was studied by means of Bristow Absorption Tester and the results being shown in Figure 33 and FibroDAT, the results being shown in Figure 34. The results from Bristow Absorption Tester showed that WTL was more sensitive to water uptake, i.e. it absorbed and spread the applied water quicker. Based on these results, where substrate A and B showed little or no water uptake, the remaining experiments used solely WTL as a substrate.

The SSE (surfactant solution/emulsion) differed by showing a fast transfer, Figure 33, which can be interpreted as fast absorption of the liquid. Similar results were achieved when spreading and absorption was studied using the dynamic adsorption tester, Figure 34. Figures 33-34 indicate together that, on a laboratory scale, SSE both spreads on and penetrates into the porous substrates most rapidly. AD spreads almost as quickly as SSE, see Figure 34 b, but it does not penetrate as quickly as SSE, see Figures 33 and 34a.
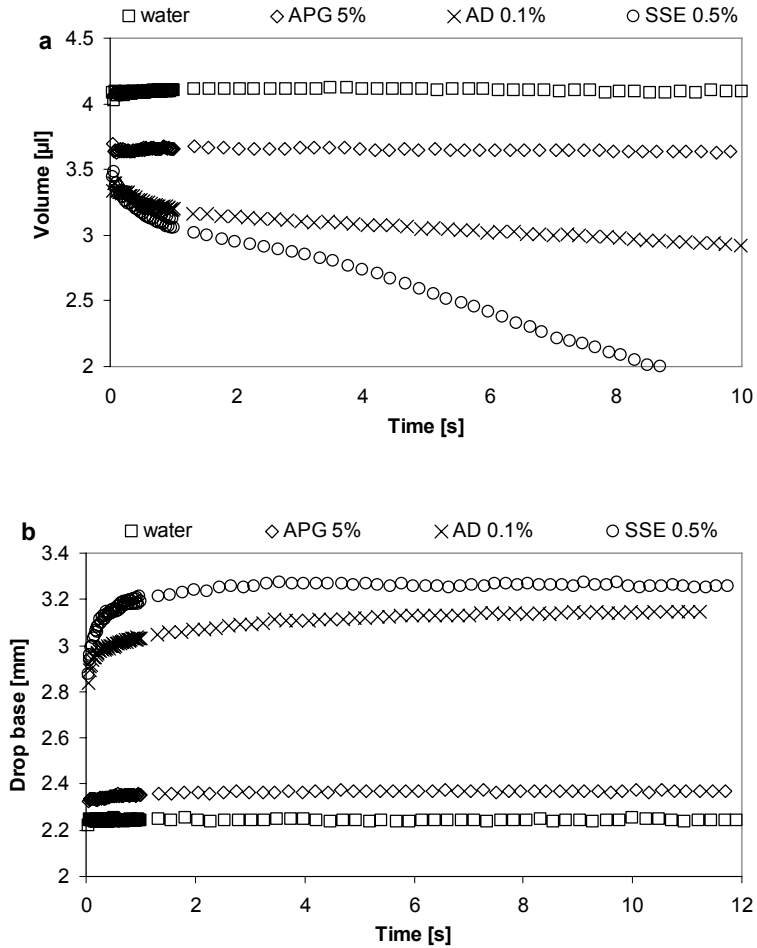
Figure 34. a) Drop volume on WTL versus time for different fluids (water, APG 5%, AD 0.1% and SSE 0.5%) using the dynamic absorption tester. b)Drop base diameter on WTL as a function of time for different fluids (water, APG 5%, AD 0.1% and SSE 0.5%) using the dynamic absorption tester.

The print was analysed with regard to mottling, Figure 35. It was found that water uptake by the substrate from ink in the previous printing units affected the final print result and it was the substrate showing the fastest wetting that showed a decrease in print mottle.
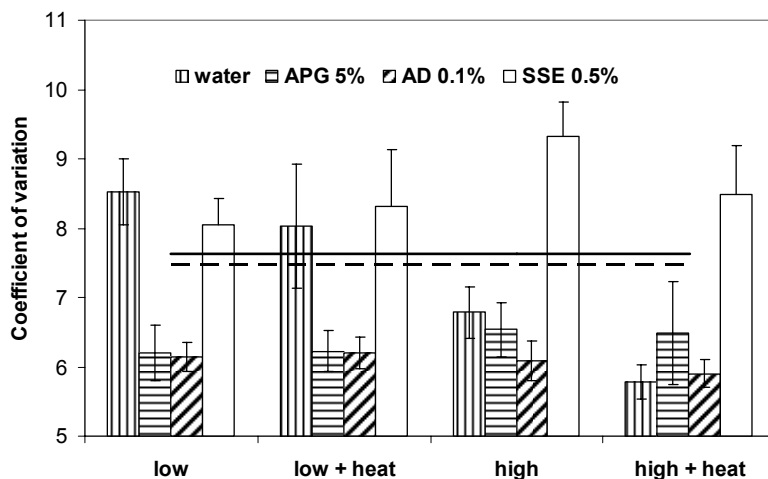
Figure 35. Mottling (1-8 mm), coefficient of variation of reflectance factor, on full-tone areas for WTL at different levels of water or model fluid application (low and high) and two levels of heat (no heat and heating power 10 kW). The solid line represents no application of water or model fluid but with heat supply (10 kW). The dashed line represents printing without application of fluid and no heat supply. The soft printing plate was used. Error bars indicate standard deviations.

The mottling in full-tone areas decreased with increased water and the influence of surfactant was also positive. The effects can be explained by the softening effect of water or by the influence of surfactant on wetting and spreading. Both surface properties and absorption of ink into the substrate affects mottling and average reflectance. The results did not unambiguously show that it was increased penetration, decreased spreading or decreased transferred of ink that have caused the variations in mottling. Viewed form the mechanical side it is water's softening effect in terms of surface compressibility that causes decreased mottling. The substrate surface becomes more flexible and co-operative with the ink covered printing plate, increasing the contact area between the two. From a chemical stand point, it is obvious that also the surface energetic of the surfactant solutions, water and substrate can affect the water uptake and spreading. Surfactant solutions and water transferred in an early printing unit can influence spreading and wetting of inks in later printing units.

71

6.2 Paper II: The Interaction between Water and Liner and Newsprint in Flexographic CI-Printing Press

This paper complements Paper I, which showed a reduction in print mottle on a white top liner (with a low water absorptivity and wettability) when, water and surfactant solution were applied just before the ink. The uncoated substrates investigated in Paper II were standard newsprint (NP) and white top test liner (TL) possessing high water absorptivity properties, and the results were compared to the findings for WTL Paper I. The substrate properties are summarized in *Table 2*, the properties of the inks in *Table 3*, the model fluids in *Table 4* and the anilox rolls, plates, tape and sleeves in *Tables 5* and *6*. The experimental set-up was the same as in Paper I and is described in *Figure 13*. The printing conditions are shown in Table 19.

Table 19. Conditions during printing in the CI-flexographic press.

Printing trial	Press room		Ink			Paper web	
	Relative humidity [%]	Temp. [ºC]	Viscosity [sec.]	Temp. [ºC]	Temp. [ºC]	Moisture content [%]	Liquid application [g/m^2]
NP							
50 m/min							
Dry	38.6	23.7	20	22.0	24.8	4.2(±0)	-
Low-water	34.9	24.2	20	22.2	24.4(±0.3)	5.8(±0)	1.2
High-water	37.8	23.5	21	21.5	23.0(±0.1)	6.9(±0)	2.4
Low-0.1 wt.-% surfynol	32.6	24.1	22	21.2	23.7(±0.2)	5.0(±0.4)	1.1
High-0.1 wt.-% surfynol	36.0	23.9	21	21.6	23.4(±0.4)	5.8(±1.5)	3.5*
100 m/min							
Dry	36.3	24.6	20	22.2	24.5(±0.1)	4.3(±0.4)	-
Low-water	34.8	24.6	20	22.4	23.7(±0.1)	6.8(±1.1)	1.3
High-water	37.5	23.8	21	21.6	23.2(±0.2)	7.6(±0.7)	2.4*
Low-0.1 wt.-% surfynol	33.2	24.1	22	21.2	23.6(±0.2)	5.9(±0.4)	1.3
High-0.1 wt.-% surfynol	37.7	23.7	22	21.5	23.1(±0.2)	7.0(±1.1)	3.2*
TL							
50 m/min							
Dry	29.9	24.4	31	23.2	23.9(±0.2)	5.0(±0)	-
Low-water	39.5	23.1	30	22.5	22.9(±0.2)	5.0(±0.6)	2.3
High-water	39.7	23.6	30	21.9	22.7(±0.2)	5.4(±0)	2.0*
Low-0.1 wt.-% surfynol	29.4	24.3	29	22.4	22.6(±0.7)	6.0(±0.3)	1.3
High-0.1 wt.-% surfynol	38.8	23.9	32	21.9	23.1(±0.4)	5.8(±0)	1.7*
100 m/min							
Dry	29.8	24.2	31	22.3	23.9(±0.2)	5.2(±0.3)	-
Low-water	39.5	23.6	30	22.0	22.6(±0.2)	5.8(±0)	1.5
High-water	40.1	23.6	30	21.7	22.5(±0.1)	6.2(±1.4)	2.2*
Low-0.1 wt.-% surfynol	30.2	24.0	29	22.0	22.1(±0.2)	7.0(±0)	1.2
High-0.1 wt.-% surfynol	39.8	24.0	32	21.8	22.6(±0.2)	6.2(±0)	2.2*

In the case of the samples denoted with an asterisk there were problems with the liquid application; the high amount of water or surfactant transported during printing did not reach the paper web satisfactorily, since some liquid "rained" through the press nip. This "rain" was collected and taken into account when the amount of applied liquid was calculated. This may explain the confusing results considering the liquid application for printing on TL at 50 m/min when applying high and low water levels; the liquid transfer determined in this case was higher when a low amount of water was applied than when a high amount was applied. In general, the measurement of moisture content showed that the higher application resulted in a higher moisture content and the lower application in a lower moisture content. Printing TL with low and high surfactant quantities was an exception; at both 50 m/min and 100 m/min, there was a higher moisture content with the low compared to the high liquid application.

The print mottle was only slightly influenced by the pre-treatment with water or surfactant solution on NP Figure 36. A low application of both water and surfactant showed a small, but insignificant, decrease in print mottle at 50 m/min. TL was not influenced to any great extent by the surfactant or water treatment. A tendency for a small, insignificant, reduction of print mottle was seen at 50 m/min and low transfer at 100 m/min. At high transfer, the print mottle was more or less the same as in the dry case. These results differ from those previously presented in Paper I for WTL, where a reduction (10%) of print mottle was seen on a white top liner when applying a large amount of water or surfactant.
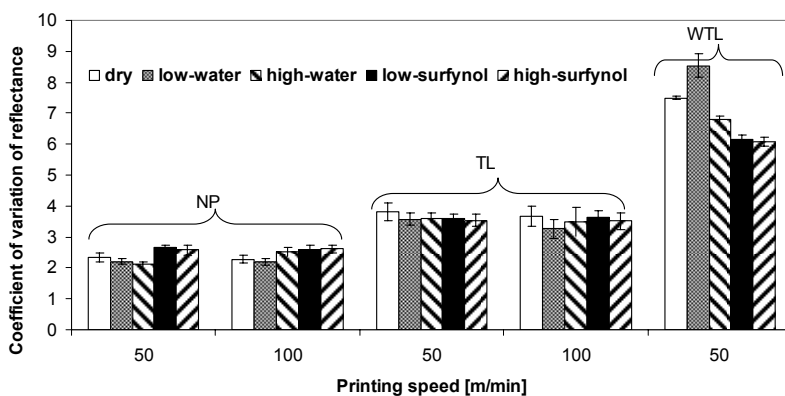
Figure 36. Print mottle (coefficient of variation in print density for the 1-8 mm wavelength range) on WTL, NP and TL treated and untreated with water or surfactant solution at two levels using 28 l/cm screen ruling. The printing speed was 50 m/min or 100 m/min, but only 50 m/min for WTL. The values for WTL are reproduced from Paper I. Error bars indicate the 0.95% confidence interval.

The interaction between the substrates and the water or the surfactant solution was studied using Bristow Absorption Tester and FibroDAT. The results are shown in *Figures 30* and *31* and showed that both the liquids were spread and absorbed on NP and TL, but no spreading or absorption were seen for WTL. This may depend on the sizing of WTL, which prevents the liquids from spreading and penetrating into the substrate. The Cobb-value indicates the degree of sizing, where lower value indicates a higher degree of sizing. WTL has a value of 24 g/m^2, whereas TL has a value of 134 g/m^2 and NP has a value of 69 g/m^2 (Table 1). The contact angle with water also indicated the more hydrophobic characteristic of WTL, where WTL possessed the highest contact angle ($\theta>90$) compared to NP and TL ($\theta<90$). The dynamic absorption tester, *Figure 31*, showed that the fastest uptake and the highest amount of liquid transferred were on TL. The lowest amount of transferred liquid was found for WTL, which also showed the slowest uptake. The fact that a certain amount of liquid was transferred to WTL using the dynamic absorption tester, even though no absorption or spreading was observed, could be attributed to the surface roughness (Bristow, 1967).

No significant improvement in print mottle in solid tones on NP and TL was seen after pre-treatment with liquids, Figure 36. Both substrates had a low surface compressibility (Table 1). In Paper I pre-treatment with a high amount (~2 g/m^2) of water reduced print mottle on white top liner (WTL). WTL, NP and TL differ in substrate properties such as surface compressibility, Cobb$_{60}$, dynamic absorption of water and contact angle with water. WTL showed no significant water absorption (drop volume) in experiments performed with the FibroDAT equipment, and the Cobb$_{60}$ value showed a high degree of surface sizing, a hydrophobic surface ($\theta > 90°$ for water) and a higher surface compressibility (at least at 23°C, 50 % RH), although the results obtained with the Bristow Absorption Tester showed that a certain amount of water was transferred to the WTL surface. Surface compressibility plays a part in ink transfer, and a higher surface compressibility leads to a more uniform print result (Hsu 1962, Blokhius and Kalff 1976, and Mangin and Geoffroy 1989).

The study showed that the water derived from the water-based ink in a previous printing unit can affect the print quality in a later printing unit. The measurements made to evaluate print quality showed that pre-treatment with water or surfactant solution had no positive effect on print mottle on the unsized newsprint (NP) or testliner (TL) substrate, both of which possessed a considerable water uptake capacity. In general print mottle for NP and TL remained unchanged or increased slightly as a result of the pre-treatment. The favorable effect that water or surfactant solution had on WTL with regard to print mottle in Paper I could depend on its surface compressibility in combination with the hydrophobic nature of its surface that could the affect wetting properties in a subsequent printing unit.

6.3 Paper III: Dynamic Nip Pressure in a CI-Flexographic Printing Press

The dynamic nip pressure in a flexographic printing press has been studied, by means of thin load cells, the aim being to measure and estimate the dynamic nip pressure at different press speeds and different impressions, using different printing plate materials and to assess its consequence for print quality on uncoated board. The substrate properties are summarized in *Table 2*, the properties of the used inks in *Table 3*, and the anilox rolls, plates, tape and sleeves in *Tables 5* and *6.*The experimental set-up is described in *Figure 14*.

The load cell was introduced into the nip between the board substrate and the printing plate cylinder, and measurements were made on the solid tone area of the printing plate. Figure 37 shows a typical pressure pulse. The maximum nip pressure data showed good agreement with experimental pressure profile data published by Mirle and Zettlemoyer (1988).
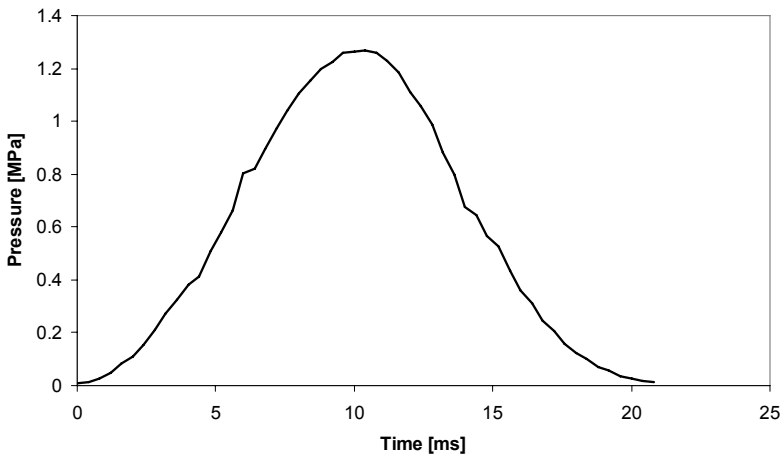

Figure 37. Typical pressure pulse at a printing speed of 50 m/min, soft printing plate and impression 200 µm.

An increase in impression led to a higher dynamic nip pressure but neither press speed nor printing plate material had any significant influence on the

maximum dynamic nip pressure. The dwell time decreased and the nip length increased with increasing web speed. *Figure 26 a* and *b* shows the maximum pressure and dwell time as a function of press speed for the "soft" and "hard" printing plates. The "hard" and "soft" printing plates and the sleeve had approximate E-moduli of 280 MPa, 420 MPa and 10 MPa, respectively, at a frequency of 100 Hz, which corresponds to a pulse time of 0.01 s with a haversine pulse according to platen press trials. The "soft" printing plate gave a higher print density than the "hard" printing plate, Figure 38. This was explained by the fact that the "soft" plate had a greater flexibility and could therefore comply better with surface asperities of the substrate, even if the main deformation occurred in the sleeve, *Figure 21*.
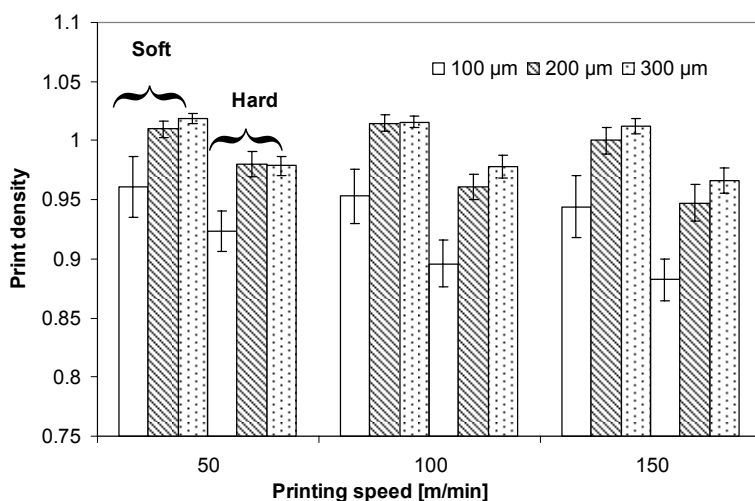

Figure 38. Print density for solid tone using "soft" and "hard" printing plate at different printing speeds (50, 100 and 150 m/min) and different impressions (100, 200 and 300 µm). Error bars indicate standard deviations.

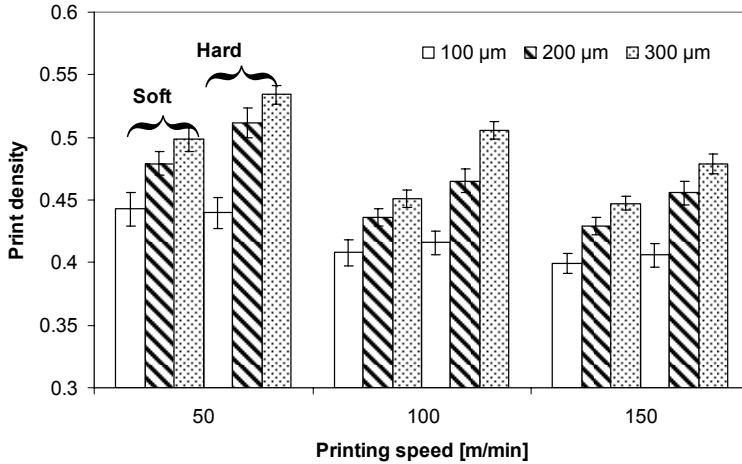Similar measurements were made on half-tone areas with a tone value of 50 % and 28 l/cm screen Figure 39.

Figure 39. Print density for halftone (tone value 50 % and screening 28 l/cm) using "soft" and "hard" printing plate at different printing speeds (50, 100 and 150 m/min) and different impressions (100, 200 and 300 µm). Error bars indicate standard deviations.

The "hard" printing gave a higher print density than the "soft" printing plate. This was interpreted as being due to a higher dot gain using the "hard" printing plate. There was a slight decrease in print density with increasing press speed, for both solid tone and half tone areas. Low impression (100 µm) gave a low print density and a low dot gain. As the pressure increased, the print density increased, and the dot gain was greater. Megat Ahmed et al. (1997) have reported that pressure, ink viscosity and initial ink thickness have an influence on dot gain. Dot gain increased with increasing film thickness and increasing pressure, but decreased with increasing ink viscosity. Both ink thickness and ink viscosity were kept constant during the printing trials, but the ink viscosity is both temperature-dependent and shear-rate-dependent, so the ink viscosity decreases with increasing temperature and increasing press speed. This may lead to changes in ink viscosities which are not taken into account here. Figure 40 shows the dot gain for the "soft" and "hard" printing plate at different impressions and different press speeds.
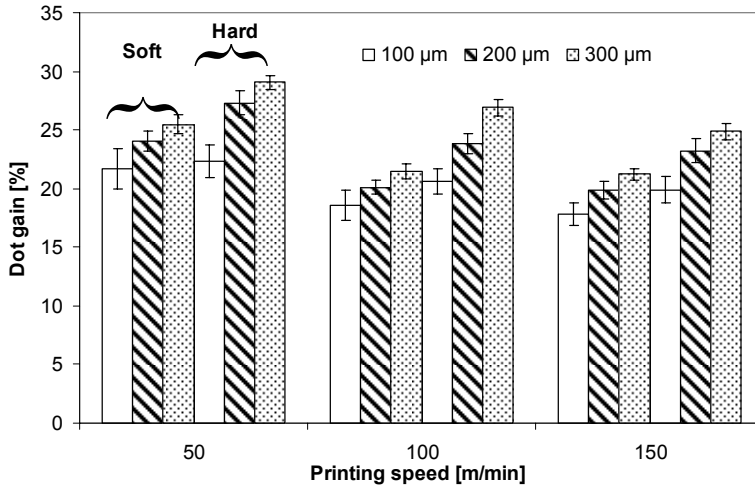
Figure 40. Dot gain for halftone (tone value 50 % and screening 28 lines/cm) using "soft" and "hard" printing plate at different printing speeds (50, 100 and 150 m/min) and different impressions (100, 200 and 300 μm). Error bars indicate standard deviations.

The highest dot gain was seen at 50 m/min. Dot gain declined with the press speed up to 100 and 150 m/min. At 50 m/min there was a long dwell time, the ink had time to spread on the substrate surface and this led to an increase in dot gain. The dot gain increased with increasing impression. The "hard" printing plate showed the same tendencies as the "soft", but generally gave a higher dot gain. The dot gain is here defined as the difference between the dot area on the film negative and the effective printed dot area. The same film negative was used for the "soft" and "hard" plates. Small differences between "soft" and "hard" (up to circa 2 %) can be explained in terms of the plate-making process.

It is possible to record the average dynamic pressure in a flexographic printing nip using thin load cells. Even though the differences in mechanical properties between the printing plates were small, they differed with regard to ink transfer and print quality. The "soft" printing plate gave a higher print density in solid tone areas, a higher ink transfer and also a smaller dot gain than the "hard" printing plate. This may be explained by the greater compliance of the "soft" printing plate which may give a better contact area between the ink-covered printing plate and the substrate.

79

6.4 Paper IV: Measuring the dynamic pressure in a flexographic central impression printing press

The dynamic pressure in a central impression flexographic printing press was measured using a thin sensor. A correction procedure taking into account the size of the sensor was developed in order to estimate the maximum dynamic pressure in the printing nip.

Since the load cell was relatively large compared with the nip length (a load cell diameter of 9.5 mm compared with a nip length of 8-14 mm) a correction procedure was required to take into account the size of the sensor. The nip length was corrected by simply subtracting the sensor length from the measured pulse length. Calculating the maximum pressure, however, needed some further evaluation.

The pressure profile was assumed to follow a cosine relationship. This assumption was made on the basis of the raw data acquired from the sensor. Thus the modelling should be regarded as a simulation of the pressure measured by the sensor rather than of the pressure experienced by substrate or ink in the nip.

$$\sigma(t) = \sigma_{max} \cdot \cos\left(\pi \cdot \frac{t}{t_p}\right) \qquad\qquad [30]$$

where σ_{max} is the maximum pressure and t_p is the length of the pressure pulse. The maximum pressure is reached in the centre of the nip where $t=0$. The pressure can be expressed as a function of distance, x:

$$\sigma(x) = \sigma_{max} \cdot \cos\left(\pi \cdot \frac{x}{a}\right) \qquad\qquad [31]$$

where a is the nip length in the printing unit. The position of the sensor in the middle of the printing nip, i.e. when the maximum pressure was reached, is illustrated in Figure 41.
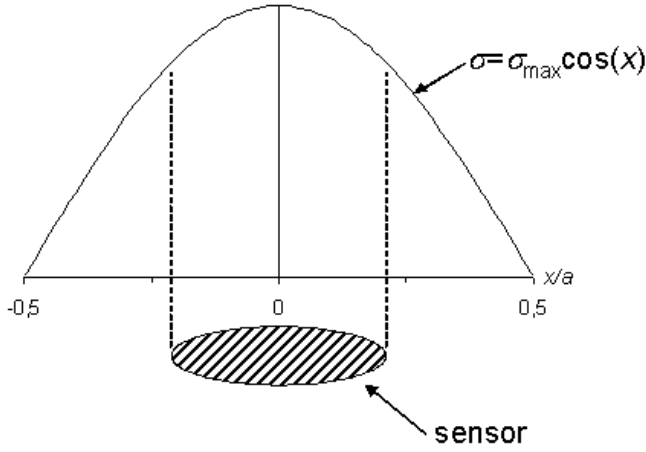
Figure 41. The pressure in the printing nip as a function of the position in the nip. The sensor is drawn below the curve to illustrate where the sensor is located when the maximum pressure is measured.

If σ^* is the measured maximum pressure, the force over the load cell at the measured maximum pressure can be calculated as:

$$F = \sigma^* \cdot A = \sigma^* \cdot \pi \cdot R^2 \qquad\qquad [32]$$

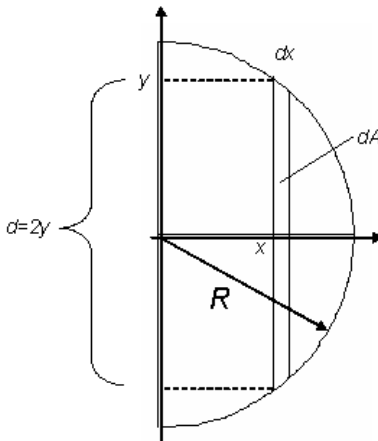where A is the area of the sensor and R is the radius of the sensor.

Figure 42. Schematic illustration of half the sensor. The area dA is given by the product of the height, d, and length, dx. R indicates the radius of the sensor.

81

Half the sensor is illustrated schematically in Figure 42. The x-direction is considered to be in the machine direction of the printing press and the y-direction is considered to be in the cross direction of the printing press. If a small area of the sensor, $dA=2\,y\cdot dx$, is considered (see Figure 42) the pressure over this area, dF, can be calculated as:

$$dF = \sigma(x)\cdot dA = \sigma(x)\cdot 2\cdot y\cdot dx \qquad\qquad [33]$$

The y-coordinate in equation [35] can be expressed as:

$$y = \sqrt{R^2 - x^2} \qquad\qquad [34]$$

Inserting equations [31] and [34] into equation [33] gives:

$$dF = \sigma_{max}\cdot \cos\left(\pi\cdot\frac{x}{a}\right)\cdot 2\cdot\sqrt{R^2 - x^2}\cdot dx \qquad\qquad [35]$$

The force on the sensor can then be calculated by integrating equation [36] over the sensor.

$$F = \sigma_{max}\cdot\int_{-R}^{R}\cos\left(\pi\cdot\frac{x}{a}\right)\cdot 2\cdot\sqrt{R^2 - x^2}\cdot dx \qquad\qquad [36]$$

Combining this result with equation [32] gives:

$$\sigma*\cdot\pi\cdot R^2 = \sigma_{max}\cdot\int_{-R}^{R}\cos\left(\pi\cdot\frac{x}{a}\right)\cdot 2\cdot\sqrt{R^2 - x^2}\cdot dx \qquad\qquad [37]$$

Rearrangement of equation [37] yields:

$$\sigma_{max} = \frac{\sigma*\cdot\pi\cdot R^2}{\int_{-R}^{R}\cos\left(\pi\cdot\frac{x}{a}\right)\cdot 2\cdot\sqrt{R^2 - x^2}\cdot dx} \qquad\qquad [38]$$

where σ^* and a can be determined from experimental data.

Figure 43 shows the maximum pressure after applying this correction procedure for the soft and the hard printing plate. An increase in impression led to a higher dynamic pressure but neither press speed nor printing plate material seemed to have any significant influence on the maximum pressure. The soft printing plate showed a clear relationship between the maximum pressure and the impression. The hard plate showed a similar relationship, but it was less pronounced when the impression increased from 200 to 300 µm.
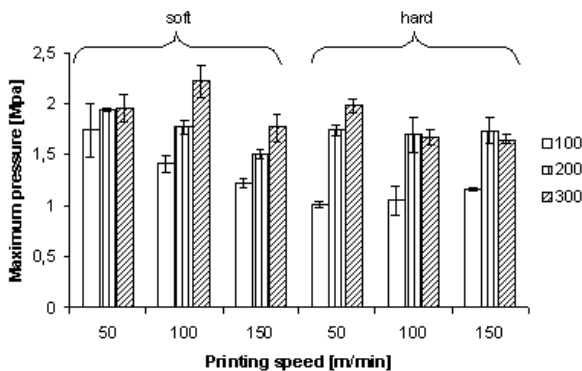

Figure 43. The maximum pressure for the soft and hard printing plates at different speeds and different impressions. The data have been processed using the correction procedure in equations [30] to [38]. The error bars show the standard deviations.

The dynamic pressure pulse in a flexographic printing press was measured and a correction procedure was developed to take into account the relatively large sensor. A higher impression led to an increase in the pressure in the printing nip. The pressure was unaffected by the printing speed. The pressure and the dwell time are important parameters for the ink transfer to the substrate, as well as the choice of material in the printing plate.

6.5   Paper V: Degradation of Flexographic Printing Plate and Aspects of Print Quality

The purpose of this paper was to analyse the effects on print quality when the properties of the flexographic printing plate were changed in a systematic and controlled way. An attempt was made to identify essential parameters of the plate that affect print quality. The parameters investigated and their values are shown in *Tables 8-11* and *13-16*. The line load was also determined. The surface energy values were not fully satisfactory and they are not discussed in this summary. One plate underwent ordinary pre-press process described in *Figure 6* and denoted norm.exp.. Some samples were over-exposed in the pre-press process with UVA and UVC radiation (*Table 7*) and denoted 2UVA, 3UVC and 4UVC. Additional samples from the ordinary pre-press process were also treated in an accelerated weather tester (*Table 7*) and denoted 2h340, 4h340, 1cy340 and 2cy340. The weather tester is shown in *Figure 23*. The results showed that it was possible to change the material properties of the plate in a systematic and controlled way.
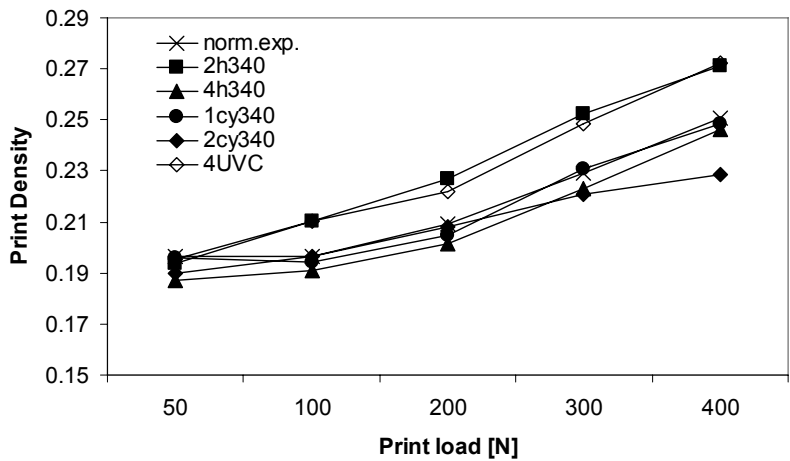

Figure 44. Print density for tone value 20% with a screen ruling of 34 l/cm using normally exposed, degraded and 4UVC plates at different printing loads.

Figure 44 shows the print density for the treated plates at different printing loads for the 20% tone value. All plates except 2h340 and 4UVC gave

roughly the same curve of print density versus printing load. The highest print density was achieved with 2h340 at nearly all printing loads. The over-exposed 2UVA and 3UVC had curves similar to those of 4UVC, and these are not shown in the figure.

Figure 45 shows the print density for samples at different printing loads for the solid tone. The print density increased with printing load for all samples except 2cy340, which showed a maximum in print density with a printing load of 200 N. This behaviour could be due to the exaggerated exposure to UVA-radiation. The highest print density was obtained with the normally exposed plate. The increase in print density was strongest from 50 N to 100 N. After 200 N, the print density reached an almost constant value particularly for normally exposed, 2h340, 4h340 and 1cy340. The over-exposed 2UVA and 3UVC had curves similar to those for 4UVC, and these are not shown in the figure.
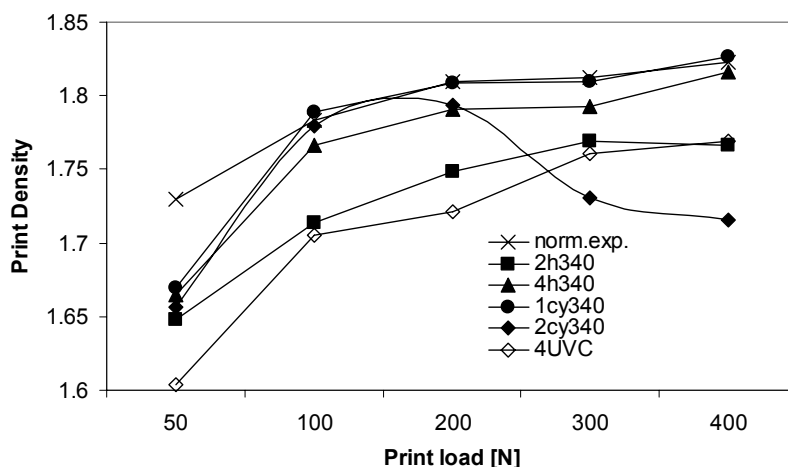

Figure 45. Print density for a full-tone area using normally exposed, degraded plates and 4UVC at different printing loads.

A multivariate analysis was adopted for the evaluation of the print quality data. Model20%PD contained the non-geometrical variables; roughness, micro-roughness, surface energy, line load and hardness and the geometrical variables: dot area on plate and dot shoulder angle. Model100%PD included only the non-geometrical variables.

85

Figure 46 shows the loading plot for print density on a half-tone area (20%). Print density increased with line load. There was less pronounced tendency for a larger dot area (within the same tone value) and a higher roughness and micro-roughness gave a higher print density. The effect of micro-roughness and roughness on print density grew stronger as the tone value increased (20 %→70 %) (not shown). A weak tendency showed that a softer dot would give a higher print density. This was contradictory to the findings in Paper III, where a hard dot achieved a high half-tone print density compared to a soft. However, the latter was printed on an uncoated substrate and the printing trials were made in a full-scale printing press, and this may explain the difference in the results. The plates were also taken from different plate manufacturers. Dot shoulder angle was placed perpendicular to print density and had no influence.
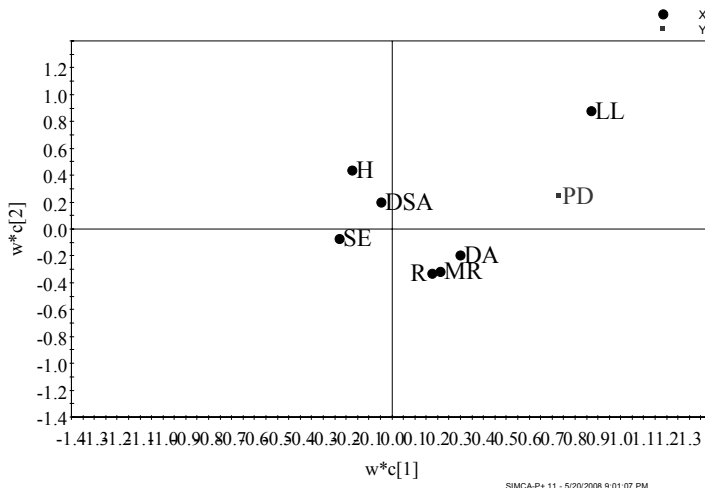

Figure 46. Loading plot w*c[2] vs. w*c[1] model20%PD. Where, PD=Print density, LL=Line load, MR=Micro-roughness, R=Roughness, H=Hardness, DSA=Dot shoulder angle, DA=Dot area and SE=Surface energy.

Figure 47 shows the loading plot for print density on a solid tone. The print density increased with increasing line load. Plate hardness did not affect the print density. There was a tendency that lower roughness gave a higher print density. Increasing micro-roughness led to a higher print density.
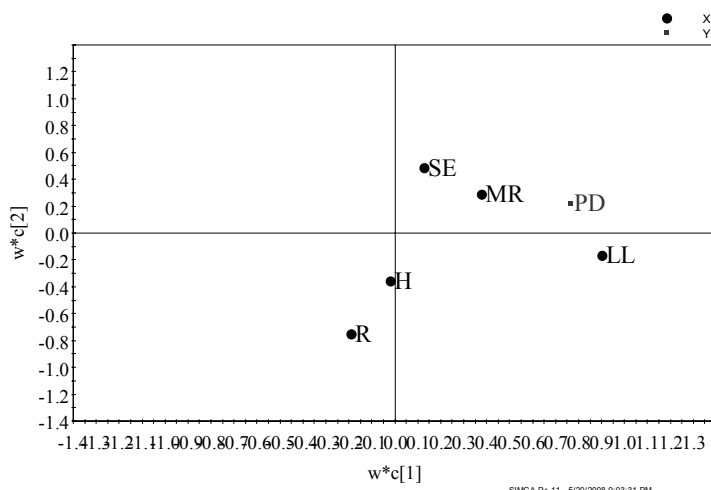
Figure 47. Loading plot w*c[2] vs. w*c[1] model100%PD. Where, PD=Print density, LL=Line load, MR=Micro-roughness, R=Roughness, H=Hardness and SE=Surface energy.

The laboratory printing results in Figure 44 and the results achieved with multivariate analysis in Figure 46 agreed that print density increases with increasing line load. This is generally a well accepted statement. The multivariate analysis also showed a tendency for the size of the dot on the plate within a tone value to influence the print density, as a larger dot led to an increase in print density. Increasing micro-roughness and roughness led to a higher print density, and the tendency was stronger as the dot became larger (not shown). Figure 44 displayed that 4UVC and 2h340 had the highest print density at every line load. The overall largest dot area, according to *Table 16*, was possessed by 4UVC, which also had the highest micro-roughness according to with *Table 8*. There was no simple explanation for sample 2h340, other than a combined effect of high dot area, micro roughness, and roughness.

The fact that an increasing line load increased the print density was also true for the solid tone. This was clearly shown both in the laboratory printing trials and in the multivariate analysis, Figure 45 and Figure 47. There was no single explanation of why the sample 2h340 and the over-exposed samples, 2UVA, 3UVC, and 4UVC had a lower print density at all line loads than the other samples. Instead the explanation has to be

87

given in terms of a combined effect of high roughness and low micro roughness. The samples 1cy340 and normally exposed gave a somewhat higher print density at same the line loads. Again this seems to be a combined effect of high micro roughness and low roughness.

Print density was increased when the line load and dot area were increased. In addition to this, micro-roughness, roughness and in some extent hardness were found to be the most significant parameters for print density using multivariate analysis. It appeared that these printing plate properties affect the amount of ink transferred. The importance of a more detailed understanding of how plate-making and handling affect the physical and chemical properties of the plate are inferred.

7   Conclusions

Applied moisture in the form of water-borne ink from an earlier printing unit can influence the print quality in a later print unit, measured as mottling. The mottling in full-tone areas decreased, on an uncoated sized hydrophobic substrate, with increasing water and the application of surfactants gave a fast wetting. The effects can be explained by the softening effect of water or by the influence of surfactant on wetting and spreading.

Print mottle remained unchanged or increased slightly for the hydrophilic unsized substrates as a result of the water-uptake. The favorable effect of water or surfactant solution seen on a hydrophobic substrate considering print mottle may depend on its surface compressibility, in combination with the hydrophobic nature of its surface that could affect the wetting properties in a subsequent printing unit.

It was possible to record the average dynamic pressure in a flexographic printing nip using thin load cells. Printing trials were performed on uncoated substrates. The "soft" printing plate gave a higher print density in solid tone areas, a higher ink transfer and also a smaller dot gain than the "hard" printing plate. This may be explained by the better compliance of the "soft" printing plate which may give a greater contact area between the ink-covered printing plate and the substrate.

The technique for measuring the dynamic nip pressure was sophisticated, as a correction procedure was developed to take into account the relatively large sensor. A higher impression led to an increase in the pressure in the printing nip, but the pressure was unaffected by the printing speed. The pressure and the dwell time are important parameters for the ink transfer to the substrate, as well as the choice of material in the printing plate.

Plates were degraded in an accelerated weather tester and over-exposed in the normal pre-press process to change the material properties in a systematic and controlled manner. These essential changes on the printing plate cause changes in print quality. Micro-roughness and roughness,

which included the waviness of the plate caused by the laser ablation step, were the most significant parameters when investigating the consequences for print density using multivariate analysis and laboratory printing trials. A more detailed knowledge of how plate making and handling affect the physical and chemical properties of the plate are required.

8   Acknowledgements

I would especially like to express thanks to my supervisor Professor Lars Järnström for his support, positive spirit and guidance throughout this work. Special thanks are also extended to the co-authors of the papers and supervisors Associate Professor Magnus Lestelius, Dr. Peter Rättö, and M. Sc. Erik Blohm for their support during these years.

Daniel Kringlund, Karl Leino, Håkan Olsson and Inga-Lill Lindqvist at BrobyGrafiska Education are also thanked for the time in their printing house and all the valuable help concerning printing trials. Personnel at Flexopartner AB acknowledged for the supply of printing plates and valuable consultation.I thank my colleagues at the Department of Chemical Engineering at Karlstad University and friends at STFI-Packforsk AB, who have made the work environment inspiring, pleasant and joyful. Thank are also extended to Dr. Göran Ström and Dr. Per-Åke Johansson STFI-Packforsk AB for the review of the work. Dr. Anthony Bristow is acknowledged for the linguistic review of this thesis, and also for valuable discussions and scientific thoughts. Dr. Anna Nestorson is acknowledged for the performance of multivariate analysis and additional discussions considering results.

I would like to express gratitude to my family, Patrik, my dearly loved, for the encouraging pep-talks and also for critical reviews of presentations made throughout the years and last but not least Klara and Julia for their unbiased love and patience with their mother.

9 Literature Cited

Andersson, C., Johnson, J. and Järnström, L. (2008): Degradation of flexographic printing plates studied by thermal and structural analysis methods, submitted to The Journal of Applied Polymer Science.

Anon (1985): Flexographic Photopolymers Plates: Elongation and Compensation, Graphic Arts Department of Uniroyal, Inc., Flexo 10(8), pp. 63-64.

Arney, J. S., Tantalo, T. and Stewart, D. (1994): The Measurement of Surface Topography of materials by Analysis of Goniometric Reflection of Light: Factors Governing Precision and Accuracy, Journal of Imaging Science and Technology, 38(5), pp. 489-494.

Aspler, J. S. (1994): A Review of Fibre Rising and Surface Roughening Effects in Paper, Journal of Pulp and Paper Science, 20(1), pp. 27-32.

Aspler, J. S., Davis, S. and Lyne, M. B. (1984): The dynamic wettability of paper Part I: The effect of surfactants, alum, and pH on self-sizing, Tappi Journal, 67(9), pp. 128-131.

Aspler, J. S, Cormier, L. and Manfred, T. (2004): Linerboard Surface Chemistry and Structure Affect Flexographic Print quality, International printing & Graphic Arts Conference, Vancouver, British Columbia, Canada, October 4-6, 2004, pp. 167-177.

Aspler, J. S., De Grâce, J. H., Béland, M.-C., Maine, C. and Piquard, L. (1993): Transfer and Setting of Water-Based Ink. Part II: pH, Water Absorbency and Uncoated Paper Structure, Journal of Pulp and Paper Science, 19(5), pp. 203-208.

Bassemir, R. and Krishnan, R. (1990): Practical applications of surface energy measurement in flexography, Flexo, 15(7), pp. 31-32, 34-36, 38-40.

Beier, W. (2001): Handbook of Print Media, Springer, Berlin, pp. 395-408.

Bennet, J. M. and Mattsson, L. (1999): Introduction to Surface Roughness and Scattering, 2nd ed., Optical Society of America, Washington, D.C., U. S. A., pp. 3, 20.

Blair, H. (2007): You Can Handle It!, Flexo 32(7), pp 36, 37, 39.

Blohm, E. and Borg, J. (2001): Methods for measuring dynamic out-of-plane dimensional stability of base paper. 2001 Coating and Graphic Arts conference and trade fair, May 6-9, San Diego, CA, U.S.A

Blokhuis, G. and Kalff, P. J. (1976): Dynamic smoothness measurements of papers and print unevenness, Tappi Journal 59(8), pp. 107-110.

Bohan, M. F. J., Townsend, P., Hamblyn, S. M., Claypole, T. C. and Gethin, D. T. (2003): Evaluation of Pressures in Flexographic Printing, Taga Proceedings, 55th annual conference, Montreal, QC, Canada, April 14-17, 2003, pp. 311-320.

Bould, D., Claypole, T. C. and Bohan M. F. J (2004): An investigation into plate deformation in flexographic printing, Proceedings of the Institution of Mechanical Engineers, Part B Journal of Engineering Manufacture, 218(11), pp1499-1511.

Bould, D., Hamblyn, S., Cherry, J. and Claypole, T. (2007): Modelling the anilox-plate micro contact, Proceedings of the 34th International Associations of Research Organizations for the Information, Media and Graphic Arts Industries, September 9-12, Grenoble, France, pp. 1-9.

Bristow, J. A. (1967): Liquid Absorption into Paper During Short Time Intervals, Svensk Papperstidning, 70(19), 623-629.

Bristow, J. A. (1982): The surface compressibility of paper, Svensk Papperstidning, 85(15), pp. 127-131.

Cushdin, G., B. (1999a): Flexography: Principles & Practices 5th ed., FFTA, Inc., NY, U.S.A vol. 1, pp. 13-18.

Cushdin, G., B. (1999b): Flexography: Principles & Practices 5th ed., FFTA, Inc., NY, U.S.A vol. 5, p. 39.

Cozzens, S. L., Butto, A. M., Schaeffer, W. D. and Zettlemoyer, A. C. (1967), Ink Penetration During High-Speed Printing of Uncoated Paper, Advances in Printing Science and Technology, Pergamon Press, Oxford, Banks, W. H. Ed., vol. 4, pp. 1-24.

Darhuber, A. A., Troian, S. M. and Wagner, S. (2001): Physical mechanisms governing pattern in microscale offset printing, Journal of Applied Physics, 90, pp. 3602-09.

De Grâce, J. H. and Mangin, P. J. (1984): A Mechanistic Approach to Ink Transfer, Part I: Effect of Substrate properties and press conditions, Advances in Printing Science and Technology, Pentech Press, London, Banks, W. H. Ed., pp. 312-332.

De Grâce, J. H. and Mangin, P. J. (1986): A Mechanistic Approach to Ink Transfer, Part II- The splitting behaviour of inks in printing nips, Pulp and Paper Reports (PPR 603), Pulp and Paper Research Institute of Canada.

Deshpande, N. V. (1978): Calculation of nip width, penetration, and pressure for contact between cylinders with elastomeric covering, Tappi Journal, 61(10), pp. 115-118.

Dullien, F. A. L (1992): Capillarity in Porous Media, 2nd ed., Academic Press, CA, U. S. A., pp. 167-177.

Etzler, F. M. and Conners, J. J. (1995): Surface analysis of Paper, CRC Press, New York, Conners, T. E and Banerjee, S. Eds., p. 98.

Fellers, C. and Norman, B. (1998): Pappersteknik, 3rd ed., Institutionen för Pappersteknik, KTH, Stockholm, Sweden, pp. 15-21, 55-65, 245, 382-387, 411-412.

Ferry, J. D. (1980): Viscoelastic properties of polymers, Wiley, New York, p. 2, 15.

Forseth, T. K., Helle, T. and Wiik, K. (1996): Surface roughening mechanism for printing paper containing mechanical pulp, International printing & Graphic Arts Conference, Minneapolis, MN, U. S. A., September 16-19, 1996, pp. 285-293.

Frøslev-Nielsen, A. (1962): The influence of printing speed and pressure on print quality, Advances in Printing Science and Technology, Pergamon press, New York, Banks, W. H. Ed., vol. 2, pp. 11-34.

Galton, D. (2003): A study of the effects of the process parameters on the characteristics of photochemical flexographic printing plates, Pigment & Resin Technology 32(4), pp. 235-247.

Grady, B. P. and Cooper, S. L. (2005): Science and technology of rubber 3rd Ed., Mark, J., Erman, B. and Eirich, R. F Eds., Elsevier Academic Press, Amsterdam, NL, pp. 604.

Hannah, M. (1951): Contact stress and deformation in a thin elastic layer, Quarterly Journal of Mechanics and Applied Mathematics, 4(1), pp. 94-105.

Hansson, P. and Johansson, P.-Å. (1999): A new method for the simultaneous measurement of surface topography and ink distribution on prints, Nordic Pulp and Paper Research Journal, 14(4), pp. 315-319.

Hansson, P. and Johansson, P. - Å. (2000): Topography and reflectance analysis of paper surfaces using a photometric stereo method, Optical Engineering, 39(9), pp. 2555-2561.

Havlínová, B., Horňáková, L., Brezová, V., Liptáková, Z., Kindernay, J. and Jančovičová, V. (2000): Ink receptivity on paper – characterization of paper materials, Colloids and Surfaces A: Physicochemical and Engineering Aspects, 168(3), pp. 251-259.

Harri, L. and Czichon, H. (2006): Microscopic Studies of the Influence of Technological Conditions on Technical Parameters of Photopolymer Flexographic Plates, Microscopy Research and Technique 69(8), pp. 675-683.

Heinemann, S. (2006): Handbook of Paper and Board, Holik, H. ed., Wiely-VCH Verlag, KGaA Weinheim, Germany, pp. 21-23.

Herzau-Gerhardt, U. (1999): Technik des Flexo drucks, Coating Verlag Thomas & Co., Gallen, pp. 1-21.

Hiemenz, P. C. (1977): Principles of Colloid and Surface Chemistry, vol. 4, Lagowski, J. J. Ed., Marcel Dekker, New York, pp. 235-240.

Hsu, B. (1962): Some Observations on the Ink-Paper Relationship During Printing, Pergamon Press, New York, Banks, W. H. Ed., vol. 2, pp. 1-10.

Istone, W. (1995): Surface analysis of Paper, CRC Press, New York, Conners, T. E and Banerjee, S. Eds., p. 235.

Johansson, K., Lundberg, P. and Ryberg, R. (1998): Grafisk kokbok, Fälth & Hässler, Värnamo, Sweden, p. 196, 210.

Johansson, P.-Å. (1999): Optical Homogeneity of Prints, Ph. D. Thesis, Royal Institute of Technology, Stockholm, Sweden.

Johnson, K. L. (1985): Contact Mechanics, University Press, Cambridge, UK, pp. 84-106.

Jönsson, B., Lindman, B., Holmberg, K. and Kronberg, B. (1998):, Surfactants and Polymers in Aqueous Solution, John Wiley & Sons, New York, pp. 247-324.

Kannurpatti, A. R. and Taylor, B. K. (2001): Taming photopolymerisation, Flexo 26(11), pp. 12-16.

Kartunnen, S. T. P. (1973): Structure and behaviour of a Paper's Surface in Printing, Bolam, F. Ed., The fundamental properties of paper related to its uses, Cambridge, UK, pp. 544-560.

Keller, S. F. (1991): Paper presented at the 77th Annual Meeting, Technical section, January 31st –February 1st, Montreal, QC, Canada, pp. 89-96.

Kenny, J. (2004): Photopolymer Plates, Label & Narrow Web 9(3), pp. 46-49.

Kilhenny, B. (2007): Restrain the Gain Cushions are Key to Control, Flexo 32(8), p. 24.

Kipphan, H. (2001): Handbook of print Media, Kipphan, H Ed., Springer, Berlin, pp. 40-59.

Laden, P. J. and Fingerman, S. (1997): Chemistry and Technology of Water based inks, 1st ed., Blackie Academic and Professional, London, pp. 220-254.

Leach, R. H. and Pierce, E. P. (1999): The Printing Ink Manual, 5th ed., Hickman, E. P., MacKenzie, M. J. and Smith, H. G. Eds., Kluwer Academic Press, London, p. 573.

Liiri-Brodén, E., Wickman, M. and Ödberg, L. (1996): Tryckfärgerskemi – en kartläggning, PFT-rapport nr. 3, pp. 7-77.

Lim, C. H., Bohan, M. F. J., Claypole, T. C., Gethin, D. T. and Roylance, B. J. (1996): A finite element investigation into a soft rolling contact supplied by a non-newtonian ink, Journal of Physics D: Applied Physics, 29(7), 1894-1903.

Liu, X. and Guthrie, J. T. (2003): A review of flexographic printing plate development, Surface Coatings International Part B: Coatings Transactions 86(B2), pp. 91-168.

Liu, X., Guthrie, J. T. and Bryant C. (2002): A study of the processing of flexographic solid-sheet photopolymer printing plates. Surface Coatings International Part B: Coatings Transactions 85(4), pp. 313-319.

Lyne, M. B. (2002): Handbook of Physical Testing of Paper, 2nd ed., vol.1, Marcel Dekker, New York, pp. 303-332.

Lyne, M. B. and Aspler, J. S. (1982): Wetting and the sorption of water by paper under dynamic conditions, Tappi Journal, 65(12), pp. 98-101.

MacPhee, J. (1998): Fundamentals of Lithographic Printing, GATFPress, Pittsburgh, pp. 86-106.

Mangin, P. J. (1986): Using the Parker Print-Surf to measure the compressibility of coated papers, Tappi Journal, 69(1), pp.90-92.

Mangin, P. J. and Geoffroy, P. (1989): Printing roughness and Compressibility: A Novel Approach based on ink transfer. Fundamentals of Papermaking, Sept. 17-22, Cambridge, UK, pp. 951-975.

Mangin, P. J., Lyne, M. B., Page, D. H. and De Grace, J. H. (1981): Ink transfer equations – parameter estimation and interpretation. Advances in Printing Science and Technology, Banks, W. H. Ed., Pentech Press, London, vol. 6, pp. 180-205.

Megat Ahmed, M. M. H., Gethin, D. T., Claypole, T. C. and Roylance, B. J. (1997): A model for ink impression into a porous substrate, Applied Physics 30, Journal of Physics D: Applied Physics, 90, pp. 2276-2284.

Micale, F. J., Iwasa, S., Sunday, S. and Fetsko, J. M. (1989): The role of wetting part 2 Flexography. American Ink Maker, 67(10), pp. 25-26, 28, 30, 32 and 35.

Mirle, S. K. and Zettlemoyer, A. C. (1987): Viscoelasticity of photopolymer plates and ink hydrodynamics in modelling flexographic printing.

Murray, A. (1936): Monochrome reproduction in photoengraving, Journal of Franklin Institute, Pergamon Press, Oxford, pp. 721-744.

Nelsen, L. E. and Landel, R. F. (1994): Mechanical Properties of Polymers and Composites, 2nd ed., Marcel Dekker, New York, pp. 33-36.

Neumann, H. (2008): (Technical Director), Flint Group, Stuttgart, Germany; personal communication.

Oum, E. (2000): "Digital" Flexo Plate Quality Unmasked, Flexo 25(10), pp. 18-20, 22, 24.

van Oss, C. J. (1994): Interfacial Forces in Aqueous Media, Marcel Dekker Inc., New York, pp. 18- 24, 175.

Parker, J. R. (1976): Fundamental Paper Properties in relation to Printability, Fundamentals properties of paper related to its uses, Bolam, F., Ed., Technical Division, The British Paper and Board Industry Federation, London, pp. 517-543.

Rodgers, B. and Wadell, W. (2005): The Science and Technology of rubber, 3rd ed., Mark, J., Erman, B. and Eirich, R. F. Eds., Elsevier Academic Press, Amsterdam, NL, p. 604.

Sharpio, F. and Sagraves, D. (1997). Chemistry and Technology of water-based inks, Laden, P. Ed., Blackie Academic & Professional, London, pp. 1-9.

Schaeffer, W. D., Fisch, A. B. and Zettlemoyer, A. C. (1963): Transfer and penetration Aspects of Ink Receptivity, Tappi Journal, 46(6), pp. 359-375.

Shaw, D. J. (2000): Colloid & Surface Chemistry, 4th ed., Butterworth Heinemann, Oxford, pp. 64-114.

Seckel, R. A. (2003): Remembering the simple basics of printing plates, Corrugating International, August, pp. 7-8.

Sheng, Y. J., Shen, W. and Parker, I. H. (1999): The importance of the surface energetics of substrate in water based flexographic printing, 53rd Appita Annual Conference Rotorua, New Zeeland, 19-23 April, vol.1, pp. 39-43.

Stemper, G. (1988): Printing Quality Begins With Accurate Plate Handling and Care, Flexo 13(5), pp. 118-121, 123-124.

Seymour, R. B. and Carraher, C. E. Jr. (1992): Polymer Chemistry, Marcel Dekker, New York, pp. 419-420.

Sutherland, J. (1982): Lithoplate photopolymer wear mechanisms, TAGA Proceedings, pp. 311-324.

Taylor, J. H. and Zettlemoyer, A. C. (1958): Hypothesis on the Mechanism of ink Splitting During Printing, Tappi Journal, 41(12), pp. 749-757.

Tillmann, O. (2006): Handbook of Paper and Board, Holik, H. ed., Wiely-VCH Verlag, KGaA Weinheim, Germany, pp. 446-466

Tollenaar, D. and Ernst, P. A. H. (1962): Optical density and ink layer thickness, Advances in Printing Science and Technology,

Banks, W. H. ed., vol. 2, Pergamon Press, London, pp. 215-234.

Toshiharu, E. and Lepoutre, P. (1999): Mechanism and dynamics of the roughening of paper in contact with moisture, 4th International Symposium on Moisture and Creep effects on paper, Board and Containers, E. F. P. G., Grenoble, France, pp. 225-233.

Trollsås, P.-O. (1995): Water uptake in newsprint during offset printing, Tappi Journal, 78(1), pp. 155-160.

Trungale, J. P. (1997): The Anilox roll, Jelmar Publishing Co., Inc., New York, pp. 33-49.

Ullman, U. and Qvarnström, I. (1976): Influence of surface smoothness and compressibility on print unevenness, Tappi Journal, 59(4), pp. 98-101.

Umetrics AB (2005): User guide and Tutorial, SIMCA-P and SIMCA-P+11.

Walker, W. C. (1981): Determination of ink transfer parameters, Tappi Journal (65(5), pp. 71-75.

Walker, W. C. and Fetsko, J. M. (1955): A concept of ink transfer in printing, American Ink Maker, 33(12), pp. 38-40, 42, 44, 69, 71.

Wasilewski, O. and Ernest, P. (1986): How Do Water Flexo News inks Differ from Oil-Based News inks And From Other Water Flexo Inks?, Flexo, 11(11), pp. 56-60.

Waterhouse, J. F. (1995): Surface analysis of Paper, CRC Press, New York, Conners, T. E and Banerjee, S. Eds., p. 72-73.

Zang, Y. –H. (1993): A new approach for modelling ink transfer. Tappi Journal, 76(7), pp. 97-103.

Zang, Y.-H. and Aspler, J. S. (1995): Factors that affect the flexographic printability of linerboards, Tappi Journal, 78(10), pp. 23-33.

Åslund, P. (2004): Dynamic Measurement measurements of water-induced roughening in paper surfaces by a new optical method, Lic. Thesis, Royal Institute of Technology, Stockholm, Sweden.

Aspects of Flexographic Print Quality and Relationship to some Printing Parameters

The thesis deals with flexographic printing on board, liner and newsprint with water-borne ink using full-scale and laboratory printing presses. Several printing trials have been performed with a focus on the chemical interaction between the ink and substrate and on the physical contact between the ink-covered printing plate and the substrate. After the first printing unit in a multicolour press, a water-containing ink is transferred to dampened surfaces in the subsequent printing units and dryers. The result showed that the water derived from the water-based ink from a previous printing unit can affect the print quality in a later printing unit.

Conventional printing involves physical contact between plate and ink and between ink and substrate. It was possible to record the dynamic nip pressure in the flexographic printing press using thin load cells. Ink transfer was influenced by the plate materials. A correction procedure taking into account the size of the sensor was developed in order to estimate the maximum dynamic pressure in the printing nip. An increase in impression led to a higher dynamic pressure but neither press speed nor printing plate material seemed to have any significant influence on the maximum pressure. The properties of the printing plate play an important role for achieving a good print. The properties of the plate that affected print quality were primarily related to the long- and micro-scale roughness of the plate.